NUREG/CR-1817
LA-8615-MS

R4

Comparison of COMPARE MOD-1 Subcompartment Calculations with Battelle-Frankfurt D-Series Test Results

J. W. Bolstad
R. G. Gido
W. S. Gregory
P. E. Littleton*
G. J. Willcutt, Jr.

Manuscript submitted: November 1980
Date published: December 1980

Prepared for
Division of Systems Integration
Office of Nuclear Reactor Regulation
US Nuclear Regulatory Commission
Washington, DC 20555

NRC FIN No. A7111

*Undergraduate Cooperative Program. New Mexico State University, Las Cruces, NM 88001.

CONTENTS

ABSTRACT 1

I. INTRODUCTION 1

II. DESCRIPTION OF THE BATTELLE-FRANKFURT D-SERIES TESTS 4

III. MODELING PROCEDURE AND ASSUMPTIONS 4
A. Volume Geometry and Initial Conditions 5
B. Junction Data. 8
C. Blowdown Data. 10

IV. COMPARISON OF COMPARE MOD-1 RESULTS WITH TEST DATA 11
A. Experiment D1. 12
B. Experiment D6. 12
C. Experiment D9. 13
D. Experiment D11 14
E. Experiment D14 15
F. Experiment D15 15
G. Summary. 16

V. MOD-2 RESULTS FOR EXPERIMENT D1. 16
A. Introduction 16
B. Problem Formulation. 17
C. Results. 17
D. Summary and Conclusions. 18

VI. PARAMETER STUDIES AND RELATED WORK 18
A. Previous Studies With COMPARE. 18
B. Sensitivity to Blowdown Fluid Quality. 19
C. Sensitivity to Inertia 20
D. Sensitivity to Noding. 21
E. Summary of Parameter Studies Performed by Others 22

VII. CONCLUSIONS AND RECOMMENDATIONS. 23
A. Conclusions. 23
B. Recommendations. 24

REFERENCES 25

APPENDIX 28

COMPARISON OF COMPARE MOD-1 SUBCOMPARTMENT CALCULATIONS WITH BATTELLE-FRANKFURT D-SERIES TEST RESULTS

by

J. W. Bolstad, R. G. Gido, W. S. Gregory,
P. E. Littleton, and G. J. Willcutt, Jr.

ABSTRACT

This report describes the results of calculations performed with the COMPARE MOD-1 and COMPARE MOD-2 computer codes. The calculations were performed for six of the Battelle-Frankfurt D-series experiments. The main emphasis of the study is to present a comparison of calculated results and experimental data. The system models used are based on regulatory rather than best-estimate assumptions. The Battelle-Frankfurt D-series tests are described and complete noding information is given for experiments D1, D6, D9, D11, D14, and D15. The main features distinguishing these tests from the others are described. Detailed comparisons between COMPARE MOD-1 calculations and experimental data are given for absolute pressure, differential pressure, and temperature at various points in the system. General trends in the comparisons are noted. Results using a method-of-characteristics approach (COMPARE MOD-2) are presented for experiment D1. These results are compared with both the MOD-1 and experimental data. Summaries of parametric studies performed using COMPARE, as well as studies performed by others, are described for the D-series experiments. Recommendations are given for assessing the conservatism in the calculations.

I. INTRODUCTION

In a loss-of-coolant accident (LOCA) within a light-water-reactor containment system, a high-energy source of water and steam will be released into the containment system. Internal structures, shielding walls, and equipment

within the containment form confined volumes that become pressurized by the break effluent build-up and flow between these volumes. These volumes are commonly referred to as subcompartments. Local transient differential pressure loadings will occur on internal structures and equipment within and between the subcompartments. Nuclear power plant safety guidelines require that subcompartment analyses be performed to determine localized containment pressure distributions that might result from high-energy-line breaks.[1] These pressure distributions may be used as input in structural analyses.

The COMPARE MOD-1[2] computer code was specifically developed to perform subcompartment transient response analyses of nuclear power plants, including those with ice condensers, and the Nuclear Regulatory Commission (NRC) recognizes it as a tool to perform such analyses. The subcompartments are represented as volumes that are connected by junctions. The volume thermodynamics and flow equations are for a homogeneous mixture assumed to be in thermodynamic equilibrium and consisting of any one or any combination of (a) steam, (b) two-phase water to its triple point, and (c) any three perfect gases such as air or helium. Flow between volumes can be based on (a) compressible (polytropic or isentropic) orifice flow of an ideal gas-like mixture that can be used to approximate the homogeneous equilibrium flow model, (b) Moody flow with an arbitrary multiplier, and (c) a one-dimensional solution of the momentum equation that includes an accounting for the effects of inertia. Variable area doors and heat sinks can also be modeled.

Briefly, COMPARE MOD-1 incorporates the following features.

- Flow and thermodynamic calculations that reflect the current state-of-art for containment subcompartment analysis.
- Thermodynamics of inert gases such as air.
- Flexibility in the selection of junction or vent flow calculation methods.
- Water thermodynamic properties down to the triple point of 273.16 k ($32.018^{o}F$).
- Representation of thermally conducting structures (heat sinks).
- Modeling of isolation doors of variable area whose opening depends on forces of pressure, springs, viscous damping, gravity, and inertia.
- Capability to model multivolume problems.

- A modular program structure to facilitate comprehension of the internal program operation and to provide a convenient framework for future improvements and additions.

Experimental verification has been a problem in assessing the accuracy of the results of subcompartment codes because test data are unavailable on geometries and thermodynamic conditions representative of those needed for subcompartment LOCA situations.

A previous study[3] was performed in which COMPARE and RELAP3 code-calculated results were compared with the Battelle-Frankfurt C-series test results. These tests used a blowdown source of saturated liquid, which introduced a two-phase mixture into the analysis. These test results were calculated using regulatory guidelines for modeling. In addition, several parametric studies were conducted to investigate the effects of (1) nodalization, (2) Moody multiplier, (3) use of the Homogeneous Equilibrium Model, and (4) entrainment. The study recommended that tests having a simpler geometric configuration and a simpler blowdown fluid, for example, series connections and air, be used to evaluate the ability of the codes to simulate simpler physical situations.

In general, computer code simulations of the C-series tests predict much higher pressures than those measured in the tests. The reason for this is not easy to determine because of the complex connections and orifice locations, the need to model two-phase flow phenomena, and the lack of some pertinent experimental data for the C-series tests. The D-series tests were devised because of these problems. The D-series tests used a steam blowdown, and several of the tests used rooms connected in series.

This study presents a comparison of computed results using COMPARE MOD-1 with test results from selected Battelle-Frankfurt D-series experiments. The emphasis is on a computer model of the system using regulatory assumptions; no attempt is made to revise the code models to produce results that agree with experiment. In addition, COMPARE MOD-2 results are presented for one of the experiments. This code is an advanced containment subcompartment analysis code using the method-of-characteristics solution procedure. This procedure should be ideal for problems that are predominately one dimensional and highly compressible. Finally, we report the results of a sensitivity analysis performed on D-series experiment D1. Sensitivity analyses of this type are reported in Refs. 3 and 4.

II. DESCRIPTION OF THE BATTELLE-FRANKFURT D-SERIES TESTS

The Battelle-Frankfurt tests involve blowdown experiments performed with a scale-model containment. The geometric scaling for the interior subcompartments and vent areas is 1:64 and is based upon a 1200-MW pressurized water reactor (PWR) plant, Biblis A. This geometric scaling allows a 1:1 scaling on the pressure histories; therefore, the test results can be extrapolated to a full-size containment in a straightforward manner.[5]

The model containment is constructed with nine inner subcompartments that are interconnected by 57 vent ducts with orifice plates of various sizes and types. Thus the system may be configured in a variety of geometries to simulate more or less complicated situations. A more complete description of the experimental apparatus is given in Refs. 3 and 5.

The D-series tests are characterized by the single-phase blowdown of approximately 69.6 bar saturated steam. Basic variations in the tests included the blowdown mass flow rate, blowdown location, subcompartments involved in the test, and the way the subcompartments were connected. Fifteen experiments, D1 through D15, were performed in the D-series tests. The earlier tests in the series were simpler (for example, D1 with 3 subcompartments) and the later tests were the most complicated (for example, D15 with 6 subcompartments).

The experimental conditions and test data obtained for the 15 tests were reviewed to select those experiments that would yield maximum information for verification of the code. Some experiments were duplicated to test the reproducibility of the experiment and to retest the measurements of important parameters. Also, some duplication was necessary to measure important parameters that were missed because of failure of the data acquisition system or its transducers. From 15 tests performed, 6 were selected for analysis. Each test (D1, D6, D9, D11, D14, and D15) is unique and represents a different level of system geometric complexity.

III. MODELING PROCEDURE AND ASSUMPTIONS

This section describes the COMPARE model for each experiment. All pertinent information is given so that others can model these experiments without

performing the preliminary hand calculations. We also list the data used for (1) volume geometry and initial conditions, (2) junction data, and (3) blowdown mass and energy rates.

A. Volume Geometry and Initial Conditions

Each node (volume) in COMPARE is assumed to contain a stagnant homogeneous mixture of steam, water, and air. To obtain information about the spatial profiles within subcompartments, the subcompartments are broken into several nodes. In general, the nodes used here were picked so that all those within a subcompartment had about the same volume (Tables I--V).

The initial temperature distributions, specified in the test reports, were about 13--22^{o}C (Tables I--V). The initial test pressures were atmospheric pressure (1 bar), which we used for all nodes, and the relative humidity was taken as 100% for all nodes.

The basic experimental configuration and COMPARE noding for experiments D1 and D6 are shown in Fig. A-1 in the Appendix. In these experiments, the blowdown source was directed into the end of room 6 (R6), and was modeled as being inserted into node 1 of the COMPARE model. Longitudinal flow existed through R6 and R4, and was directed into the receiver volume R9. The volume of each COMPARE node and its corresponding initial temperature are shown in Table I for experiments D1 and D6. The principal difference between these experiments is that experiment D1 had 0.6-m nozzles as vents between the rooms, and experiment D6 has 0.75-m orifices. The blowdown mass flow rates were also different.

TABLE I

NODING INFORMATION AND INITIAL TEMPERATURES FOR EXPERIMENTS D1 AND D6

Node	Volume (m^3)	Initial Temperature (^{o}C)
1	8.239	13.2
2	8.239	13.2
3	8.239	13.2
4	8.239	13.2
5	8.239	13.2
6	2.8	13.2
7	2.8	13.2
8	2.8	13.2
9	2.8	13.2
10	550.0	13.2

TABLE II

NODING INFORMATION AND INITIAL TEMPERATURES FOR EXPERIMENT D6

Node	Volume (m^3)	Initial Temperature (^{o}C)
1	8.252	22.1
2	8.252	22.1
3	8.252	22.1
4	8.252	22.1
5	8.252	22.1
6	8.106	22.1
7	8.106	22.1
8	8.106	22.1
9	8.106	22.1
10	8.106	22.1
11	1.347	22.9
12	1.347	22.9
13	1.347	22.9
14	480.0	23.6
15	1.032	22.1

TABLE III

NODING INFORMATION AND INITIAL TEMPERATURES FOR EXPERIMENT D11

Node	Volume (m^3)	Initial Temperature (°C)
1	8.252	19.8
2	8.252	19.8
3	8.252	19.8
4	8.252	19.8
5	8.252	19.8
6	8.21	19.1
7	8.21	19.1
8	8.21	19.1
9	8.21	19.1
10	8.21	19.1
11	8.08	19.1
12	8.08	19.1
13	8.08	19.1
14	8.08	19.1
15	8.08	19.1
16	1.197	19.1
17	3.934	19.1
18	3.934	19.1
19	3.934	19.1
20	490.53	18.4

TABLE IV

NODING INFORMATION AND INITIAL TEMPERATURES FOR EXPERIMENT D14

Node	Volume (m^3)	Initial Temperature (°C)
1	8.252	12.3
2	8.252	12.3
3	8.252	12.3
4	8.252	12.3
5	8.252	12.3
6	8.21	12.5
7	8.21	12.5
8	8.21	12.5
9	8.21	12.5
10	8.21	12.5
11	8.08	10.6
12	8.08	10.6
13	8.08	10.6
14	8.08	10.6
15	8.08	10.6
16	1.197	11.7
17	3.934	11.7
18	3.934	11.7
19	3.934	11.7
20	8.106	11.7
21	8.106	11.7
22	8.106	11.7
23	8.106	11.7
24	8.106	11.7
25	450.0	10.7

TABLE V

NODING INFORMATION AND INITIAL TEMPERATURES FOR EXPERIMENT D15

Node	Volume (m^3)	Initial Temperature (°C)
1	7.52	19.9
2	3.76	19.9
3	9.91	19.9
4	10.03	19.9
5	10.03	19.9
6	0.882	19.6
7	9.946	19.6
8	9.2	19.6
9	9.449	19.6
10	11.935	19.6
11	12.296	20.0
12	11.292	20.0
13	11.292	20.0
14	5.521	20.0
15	1.197	19.9
16	2.347	19.9
17	2.31	19.9
18	6.207	19.9
19	6.506	20.1
20	9.011	20.1
21	9.011	20.1
22	9.011	20.1
23	7.509	20.1
24	214.9	20.0
25	235.1	20.0

The basic experimental configuration and COMPARE noding for experiment D9 are shown in Fig. A-2. The blowdown source was directed into R6 and was modeled as being inserted into node 1 of the COMPARE model. This test featured a four-subcompartment chain-type arrangement: R6 (longitudinal flow) to R8 (longitudinal flow) to R7 (transverse flow) to R9. The test used

- four subcompartments,
- overflow from R6 to R8 through a channel (0.74-m diam by 2.05-m long),

- overflow from R8 to R7 and R7 to R9 through 0.75-m orifices, and
- transverse flow through subcompartment R7.

The volume of each COMPARE node and its corresponding initial temperature are shown in Table II.

The basic experimental configuration and COMPARE noding for experiment D11 are shown in Fig. A-3. The blowdown in this experiment was directed into R6 and node 5 of the model. This test featured a five-subcompartment chain-type arrangement: R6 (transverse flow) to R5 (transverse flow) to R7 (longitudinal flow) to R4 (transverse flow) to R9. There were

- five subcompartments,
- transverse flow in the break compartment (R6) and the following compartment (R5), and
- all overflow cross sections were 0.75-m orifices.

The volume of each COMPARE node and its corresponding initial temperature are shown in Table III.

The basic experimental configuration and COMPARE noding for experiment D14 are shown in Fig. A-4. The blowdown is in R5 and node 10 of the model. This test had featured a six-subcompartment arrangement with both series and parallel flow paths; longitudinal flow in subcompartments R5 and R7, transverse flow in subcompartments R6 and R8, and a combination of both in subcompartment R4. The experiment featured

- six-subcompartment series and parallel arrangement,
- overflow from R5 to R7 through 0.388-m orifice,
- overflow from R5 to R4 through 0.75-m orifice,
- overflow from R4 to R8 through 0.53-m orifice,
- overflow from R6 to R9 through 0.49-m orifice, and
- overflow from R4 to R6 and R8 to R9 through 0.424-m orifices.

The volume of each COMPARE node along with its corresponding initial temperature are shown in Table IV.

The results of experiment D15 formed the basis for an international Containment Analysis Standard Problem (CASP) for verification of containment

codes. The basic configuration of the test and its corresponding COMPARE nodding are shown in Fig. A-5. The blowdown source was injected into room 6 (node 1 of the COMPARE model), this test featured a five-subcompartment series flow arrangement: R6 to R8 to R7 (all with longitudinal flow) to R4 (transverse flow) to R5 (longitudinal flow) to R9. This test featured

- overflow from R6 to R8 through a channel (0.74-m diam by 2.05-m long)
- overflow through the remaining rooms via 0.75-m diam orifices.

The volume of each COMPARE node and its corresponding initial temperature are shown in Table V. The main reason for the nonuniform node size is that our model was originally set up to analyze the C-series tests and the nodes were located relative to potential data measurement locations.

B. Junction Data

Extensive junction data needed to run COMPARE include

- node number of the two adjacent nodes (denoted NV1 and NV2),
- area at the plane of connection between the two adjacent nodes, preferably the minimum flow area,
- entrance loss coefficient for flow from the NV1 volume to the junction (ENLK12),
- exit loss coefficient for flow from the junction to the NV2 volume (EXLK12),
- entrance loss coefficient for flow from the NV2 volume to the junction (ENLK21),
- exit loss coefficient for flow from the junction to the NV1 volume (EXLK21), and
- sum of the inertia term (L/A) for half-volumes adjacent to the junction.

The values used for these parameters are shown in Tables VI--XI.

The junction area used is the actual geometric flow area at the plane of connection between the adjacent nodes. The head losses comprise entrance and exit losses if the junction coincides with an area change, and wall friction losses. The entrance and exit losses are estimated from standard formulas for

TABLE VI

JUNCTION DATA FOR EXPERIMENT 01

Junction	NV1	NV2	Area (m²)	ENLK 12	EXLK 12	ENLK 23	EXLK 23	1/P (m⁻¹)
1	1	2	4.167	0.011	0.011	0.011	0.011	0.4746
2	2	3	4.167	0.011	0.011	0.011	0.011	0.4746
3	3	4	4.167	0.011	0.011	0.011	0.011	0.4746
4	4	5	4.167	0.011	0.011	0.011	0.011	0.4746
5	5	6	0.2627	0.018	1.019	0.019	1.018	2.136
6	6	7	2.31	1.156	0.006	0.006	2.154	1.547
7	7	8	2.31	0.008	0.008	0.008	0.008	0.529
8	8	9	2.31	0.008	0.008	0.008	0.008	0.529
9	9	10	0.2627	0.015	1.008	0.008	1.011	1.7

TABLE VII

JUNCTION DATA FOR EXPERIMENT 02

Junction	NV1	NV2	Area (m²)	ENLK 12	EXLK 12	ENLK 23	EXLK 23	1/P (m⁻¹)
1	1	2	4.167	0.011	0.011	0.011	0.011	0.4746
2	2	3	4.167	0.011	0.011	0.011	0.011	0.4746
3	3	4	4.167	0.011	0.011	0.011	0.011	0.4746
4	4	5	4.167	0.011	0.011	0.011	0.011	0.4746
5	5	6	0.4418	0.518	1.019	0.519	1.018	2.137
6	6	7	2.31	1.156	0.006	0.006	1.154	1.547
7	7	8	2.31	0.008	0.008	0.008	0.008	0.529
8	8	9	2.31	0.008	0.008	0.008	0.008	0.529
9	9	10	0.4418	0.515	1.008	0.509	1.011	1.7

TABLE VIII

JUNCTION DATA FOR EXPERIMENT 04

Junction	NV1	NV2	Area (m²)	ENLK 12	EXLK 12	ENLK 23	EXLK 23	1/P (m⁻¹)
1	1	2	4.11	0.011	0.011	0.011	0.011	0.4706
2	2	3	4.11	0.011	0.011	0.011	0.011	0.4706
3	3	4	4.11	0.011	0.011	0.011	0.011	0.4706
4	4	5	4.11	0.011	0.011	0.011	0.011	0.4706
5	5	15	0.43	0.462	0.022	0.022	0.732	3.0641
6	6	7	4.11	0.011	0.011	0.011	0.011	0.4706
7	7	8	4.11	0.011	0.011	0.011	0.011	0.4706
8	8	9	4.11	0.011	0.011	0.011	0.011	0.4706
9	9	10	4.11	1.161	0.011	0.011	1.161	0.4706
10	10	13	0.442	0.523	1.176	0.524	1.021	3.745
11	11	12	4.049	0.033	0.033	0.033	0.033	1.3359
12	12	13	4.041	0.033	0.033	0.033	0.033	1.3359
13	13	14	0.442	0.516	1.008	0.508	1.018	0.8133
14	15	6	0.43	0.022	0.732	0.462	0.022	3.0641

TABLE IX

JUNCTION DATA FOR EXPERIMENT 03

Junction	NV1	NV2	Area (m²)	ENLK 12	EXLK 12	ENLK 23	EXLK 23	1/P (m⁻¹)
1	1	2	4.11	0.011	0.011	0.011	0.011	0.4706
2	2	3	4.11	0.011	0.011	0.011	0.011	0.4706
3	3	4	4.11	0.011	0.011	0.011	0.011	0.4706
4	4	5	4.11	0.011	0.011	0.011	0.011	0.4706
5	5	10	0.442	0.521	1.020	0.520	1.021	3.9849
6	6	7	4.002	0.016	0.016	0.016	0.016	0.6841
7	7	8	4.002	0.016	0.016	0.016	0.016	0.6841
8	8	9	4.002	0.016	0.016	0.016	0.016	0.6841
9	9	10	4.002	0.016	0.016	0.016	0.016	0.6841
10	10	11	0.442	0.515	1.019	0.515	1.015	1.8452
11	11	12	4.002	0.016	0.016	0.016	0.016	0.6841
12	12	13	4.002	0.016	0.016	0.016	0.016	0.6841
13	13	14	4.002	0.016	0.016	0.016	0.016	0.6841
14	14	15	4.002	0.016	0.016	0.016	0.016	0.6841
15	15	19	0.442	0.515	1.021	0.521	1.015	1.9642
16	16	17	1.26	0.039	0.039	0.039	0.039	1.4539
17	17	18	2.31	0.021	0.021	0.021	0.021	0.6999
18	18	19	2.31	0.021	0.021	0.021	0.021	0.6999
19	19	20	0.442	0.517	1.006	0.508	1.017	1.5036

TABLE X

JUNCTION DATA FOR EXPERIMENT 04

Junction	NV1	NV2	Area (m²)	ENLK 12	EXLK 12	ENLK 23	EXLK 23	1/P (m⁻¹)
1	1	2	4.11	0.011	0.011	0.011	0.011	0.4706
2	2	3	4.11	0.011	0.011	0.011	0.011	0.4706
3	3	4	4.11	0.011	0.011	0.011	0.011	0.4706
4	4	5	4.11	0.011	0.011	0.011	0.011	0.4706
5	17	5	0.141	0.026	1.023	0.023	1.026	4.3077
6	6	7	4.002	0.016	0.016	0.016	0.016	0.6841
7	7	8	4.002	0.016	0.016	0.016	0.016	0.6841
8	8	9	4.002	0.016	0.016	0.016	0.016	0.6841
9	9	10	4.002	0.016	0.016	0.016	0.016	0.6841
10	10	11	0.118	0.502	1.021	0.501	1.021	4.7119
11	11	12	4.002	0.016	0.016	0.016	0.016	0.6841
12	12	13	4.002	0.016	0.016	0.016	0.016	0.6841
13	13	14	4.002	0.016	0.016	0.016	0.016	0.6841
14	14	15	4.002	0.016	0.016	0.016	0.016	0.6841
15	6	19	0.442	0.515	1.021	0.521	1.015	4.1964
16	16	17	1.26	0.039	0.039	0.039	0.039	1.4539
17	17	18	2.31	0.021	0.021	0.021	0.021	0.6999
18	18	19	2.31	0.021	0.021	0.021	0.021	0.6999
19	17	24	0.221	0.524	1.020	0.520	1.024	3.1048
20	20	21	4.11	0.011	0.011	0.011	0.011	0.4706
21	21	22	4.11	0.011	0.011	0.011	0.011	0.4706
22	22	23	4.11	0.011	0.011	0.011	0.011	0.4706
23	23	24	4.11	0.011	0.011	0.011	0.011	0.4706
24	24	25	0.141	0.028	1.013	0.023	1.008	4.0625
25	5	25	0.189	0.527	1.011	0.513	1.027	3.1019

TABLE XI

JUNCTION DATA FOR EXPERIMENT 05

Junction	NV1	NV2	Area (m²)	ENLK 12	EXLK 12	ENLK 23	EXLK 23	1/P (m⁻¹)
1	1	2	4.17	0.0075	0.0075	0.0075	0.0075	0.3214
2	2	3	4.17	0.009	0.009	0.009	0.009	0.3856
3	3	4	4.17	0.013	0.013	0.013	0.013	0.5567
4	4	5	4.17	0.0135	0.0135	0.0135	0.0135	0.5782
5	5	6	0.43	0.5135	0.024	0.024	0.0135	2.3564
6	6	7	0.43	0.024	1.0135	0.5135	0.024	2.3564
7	7	8	4.17	0.013	0.013	0.013	0.013	0.5782
8	8	9	4.17	0.012	0.012	0.012	0.012	0.5141
9	9	10	4.17	0.014	0.014	0.014	0.014	0.6011
10	10	11	0.442	0.5164	1.0149	0.5149	1.0164	1.5641
11	11	12	4.04	0.0145	0.0145	0.0145	0.0145	0.6499
12	12	13	4.04	0.0135	0.0135	0.0135	0.0135	0.6052
13	13	14	4.04	0.01	0.01	0.01	0.01	0.4496
14	15	16	1.26	0.0105	0.0105	0.0105	0.0105	0.8654
15	16	17	2.31	0.008	0.008	0.008	0.008	0.5019
16	17	18	2.31	0.0115	0.0115	0.0115	0.0115	0.7511
17	14	18	0.442	0.5091	1.0094	0.5094	1.0091	0.7220
18	18	19	0.442	0.5094	1.0101	0.5101	1.0094	0.7466
19	19	20	4.04	0.0095	0.0095	0.0095	0.0095	0.4666
20	20	21	4.04	0.011	0.011	0.011	0.011	0.5401
21	21	22	4.04	0.011	0.011	0.011	0.011	0.5401
22	22	23	4.04	0.01	0.01	0.01	0.01	0.1961
23	23	24	0.442	0.5169	1.0035	0.5035	1.0169	0.8644
24	24	25	23.12	0.047	0.047	0.047	0.047	0.3253

incompressible flow.[6] The wall friction losses were based on a Blasius friction factor of 0.02 used in the Darcy equation. Entrance and exit losses listed in the tables include the wall friction losses for the adjacent nodes. In general, flow losses between nodalized volumes of a subcompartment are dominated by the wall friction losses, whereas the flow losses at junctions corresponding to an area change are usually dominated by expansion and contraction losses. The L/A values are based on actual geometry for the flow path of the half-volumes on either side of the junction. Each L/A value listed in the tables is the sum of L/A for the constant area flow paths associated with a junction.

The vent flow option selected for these calculations is flow with inertia (KJUN = 3) with a Moody multiplier of 0.6.[2] These assumptions are in accordance with licensing calculations.

C. Blowdown Data

The blowdown mass and energy sources used in these calculations are shown in Tables XII--XVII. The blowdown mass flow rate is given as a function of time in the experiment test reports. The energy source rate is calculated as the product of the given mass flow rate and enthalpy of the fluid (given). COMPARE obtains values at arbitrary times from such tables.

TABLE XII

BLOWDOWN DATA FOR EXPERIMENT D1

Time (s)	Mass rate (kg/s)	Energy rate (Mw)
0.0	0.0	0.0
0.02	72.4	200.8
0.05	84.6	237.4
0.075	86.6	240.2
0.1	82.4	228.6
0.2	71.4	198.1
0.3	57.8	160.3
0.5	49.9	138.4
1.0	45.3	125.7
1.5	43.1	119.6
2.0	41.4	114.8
3.0	36.8	102.1

TABLE XIII

BLOWDOWN DATA FOR EXPERIMENT D6

Time (s)	Mass rate (kg/s)	Energy rate (Mw)
0.0	0.0	0.0
0.02	80.7	223.8
0.05	93.0	258.0
0.06	94.5	262.1
0.075	85.0	235.8
0.1	81.7	226.6
0.2	81.7	226.6
0.3	79.2	219.7
0.5	76.6	212.5
1.0	72.5	201.1
1.68	63.3	175.6
1.85	48.2	111.8
2.0	131.7	161.8
2.5	130.2	177.3
2.7	132.6	184.0
4.0	121.4	171.4

TABLE XIV

BLOWDOWN DATA FOR EXPERIMENT D9

Time (s)	Mass rate (kg/s)	Energy rate (MW)
0.0	0.0	0.0
0.02	77.0	213.6
0.05	85.3	236.6
0.07	88.8	246.3
0.1	78.9	218.9
0.125	76.7	212.8
0.2	67.6	187.5
0.3	57.8	160.3
0.5	50.2	139.3
1.0	43.3	120.1
1.5	41.0	113.7
2.0	39.2	108.7
2.5	37.6	104.3
2.97	36.0	99.9
3.14	26.1	72.4

TABLE XV

BLOWDOWN DATA FOR EXPERIMENT D11

Time (s)	Mass rate (kg/s)	Energy rate (MW)
0.0	0.0	0.0
0.008	0.0	0.0
0.02	70.5	195.6
0.06	80.8	224.1
0.1	73.7	204.4
0.2	60.3	167.3
0.3	53.9	149.5
0.4	49.4	137.0
0.5	47.4	131.5
1.0	42.3	117.3
2.5	36.5	101.3
2.75	35.9	99.6
2.9	19.8	54.9

TABLE XVI

BLOWDOWN DATA FOR EXPERIMENT D14

Time (s)	Mass rate (kg/s)	Energy rate (MW)
0.0	0.0	0.0
0.008	0.0	0.0
0.07	85.5	237.2
0.32	57.5	159.5
0.72	47.4	131.5
1.0	44.8	124.3
2.8	37.8	104.9
2.95	28.2	78.2

TABLE XVII

BLOWDOWN DATA FOR EXPERIMENT D15

Time (s)	Mass rate (kg/s)	Energy rate (MW)
0.0	0.0	0.0
0.007	0.0	0.0
0.015	70.0	194.1
0.025	82.0	227.4
0.06	88.0	244.0
0.09	77.0	213.1
0.15	74.0	204.5
0.30	57.0	157.1
0.55	47.0	129.5
0.75	45.0	123.9
2.8	38.0	103.5
2.95	26.0	70.8
3.0	60.0	88.7
4.0	73.0	108.5
6.0	57.0	91.5
10.0	40.0	76.7

IV. COMPARISON OF COMPARE MOD-1 RESULTS WITH TEST DATA

This section presents the results of the COMPARE MOD-1 calculations along with the experimental data for comparison. For most of the experiments, the duration of steam admission into the containment is approximately 3 s and short-term experimental data are available for 0 to 2.5 s; therefore, we show the results for the first 2.5 s of the blowdown transient. The results show that

this time scale includes the phenomena of primary interest, that is, the time of the maximum pressure differential between rooms.

Available data from the test reports[7--12] (differential pressures, absolute pressures, and temperatures) are compared for each room; however, subcompartment R9 is not noded to give detailed temperature histories, so that value is unavailable for comparison. The experimental data shown in this report for comparison purposes are typical data when many measurements are taken in a given volume. In general, the experimental data traces shown are smoothed, but some oscillations are shown for display purposes. Therefore, in general, the data scatter and uncertainty are not shown on the experimental plots; however, more detailed information is available in the experimental reports.[7--12]

One of the major concerns regarding subcompartment analysis codes is the adequacy of the critical flow model used. The D-series tests do not allow a detailed analysis of critical flow models because the tests were at low pressure, and, in general, pressure ratios were less than 1.2. Therefore, critical flow did not occur in these tests.

A. Experiment D1

Figures A-6--8 show the calculated and experimental absolute pressures for R6, R4, and R9. The calculations overpredict the measured pressures for all three rooms, with the greatest overprediction in blowdown room R6, and the smallest in containment room R9.

The calculated and experimental differential pressures between the three rooms are shown in Figs. A-9--11. The calculated differential pressures are higher than the measurements, with the larger difference across the second orifice (R4 to R9).

Figures A-12 and A-13 show that calculated temperatures were higher than measured temperatures. Actual measurements show saturation temperature for the existing room pressures, whereas the calculated temperatures are approximately $50^{o}C$ superheated after a short time.

B. Experiment D6

Although Figs. A-14--16 show that the calculated pressures are generally higher than the measured absolute pressures for R6, R4, and R9, the agreement is closer than it was for experiment D1. The decrease in pressure between 1.7

and 2.0 s is due to a decrease in the blowdown mass flow rate (as indicated in Table XIII) during this time.

The calculated and experimental differential pressures for the three rooms are shown in Figs. A-17--19. Agreement is excellent between calculation and experiment for the differential pressure between R6 and R4. At the same time, the difference between calculation and measurement between R4 and R9 is about the same as in experiment D1 at the time of maximum differential pressure ($\sim$0.5 s). (Remember that the principal difference between experiments D1 and D6 is the vent geometry.)

Figures A-20 and A-21 show that, as in experiment D1, the calculated room temperatures are higher than the measured temperatures; however, at 1.7 s (when the blowdown mass flow rate decreases), the calculated temperature in R6 quickly decreases to saturation temperature, and thereafter is in excellent agreement with the measurement. The same behavior is exhibited in R4 approximately 0.4 s later.

C. Experiment D9

Figures A-22--25 show the calculated and experimental absolute pressures for the four rooms. The figures show the calculated pressure to be higher than the measured pressure. In general, the results are similar to those shown for the previous experiments, except that the calculated pressure in the containment is lower than that measured for the first second, and the agreement between the calculation and the measured value is better over the entire 2.5 s.

The calculated and experimental differential pressures between R7, R8, and R9 are shown in Figs. A-26--28. The experimental pressure differentials among these three rooms are essentially zero, but the calculated pressure differentials are significant. This is probably caused by the jet effect, which occurs between R8 and R9 because of the straight-through geometry (see Fig. A-2). No attempt is made to account for this effect in the present calculational tool and good agreement is not expected. The calculated overall differential pressure between R6 and R9 is higher than measured, as shown in Fig. A-29.

The calculated and experimental temperatures for R6, R8, and R7 are shown in Figs. A-30--32. The calculated temperatures are much higher than experiment for R6 and R8, whereas the calculated temperature in node 12 of R7 is much closer to experiment. The much lower temperature in node 12 is because it is a

stagnant volume and very little steam flows into it as there is no longitudinal flow through R7. In this arrangement, large temperature differences will occur between nodes 12 and 13 (Fig. A-2), but at the same time, flow or pressure differences between these nodes will be small.

D. Experiment D11

Calculated and experimental absolute pressures for the five rooms are shown in Figs. A-33--37. Calculated pressures in R5 and R6 are very close to the experimental measurements, unlike the other tests where calculated blowdown volume pressure is significantly higher than that measured. Calculated pressures in R7, R4, and R9 are higher than the measurements, but the agreement is quite good.

Experimental pressure differentials are shown with corresponding calculated values in Figs. A-38--42. Note the excellent agreement between calculated and measured pressure differentials between R5 and R6 shown in Fig. A-38. It is interesting to note that the only other pressure differential plot that shows such good agreement is for test D6 (Fig. A-17). The common characteristic in these two experiments is that both have 0.75-m-diam orifices for the overflow cross section. Figure A-39 shows very good agreement for the pressure differentials between R5 and R7 as well. Figure A-40 illustrates an unusual result; the calculated pressure differential is less than the measured pressure differential, although the difference between the two is small. This is the only example of such behavior in all the comparisons. The calculated pressure differential between R4 and R9 (Fig. A-41) is higher than that measured. The calculations have underpredicted the differential pressure between R7 and R4 and over-predicted that between R4 and R9. However, note that the net effect is almost perfect agreement for the pressure differentials between R7 and R9 shown in Fig. A-42. As in experiment D9, we felt that the discrepancy in the pressure differential comparisons was caused by the jet effect, which occurs between R5, R7, and R4 because of the straight-through geometry (Fig. A-3). This effect is not accounted for in the COMPARE code, and good agreement is not expected for this type of geometry.

The calculated and measured temperatures for R6, R5, R7, and R4 are shown in Figs. A-43--46. Fairly good agreement was obtained in R6, R5, and R4, which have stagnant volumes. At the same time, the calculated temperature for R7,

which had transverse flow conditions (Fig. A-45), is much higher than measured. This is the same phenomenon that was discussed for test D9.

E. Experiment D14

The calculated and experimental absolute pressures for the six rooms are shown in Figs. A-47--52. In general, the calculated pressures are higher than the measured pressures; however, the agreement is quite good at early times for R6 (Fig. A-50), and is quite good at all times for R9 (Fig. A-52). We noted a nonsymmetric pressure distribution in R6 and R8, located in parallel branches of the flow path. This occurred in the experimental data as well.

Calculated and experimental differential pressures are shown in Figs. A-53--59. Good agreement is obtained for the differential pressures between R7 and R5 (Fig. A-53), R4 and R5 (Fig. A-54), R4 and R8 (Fig. A-56), and R4 and R7 (Fig. A-59). The calculated pressure differential is higher than measured between R4 and R6 (Fig. A-55), R6 and R9 (Fig. A-57), and R8 and R9 (Fig. A-58). It is interesting that the larger overpredictions occurred at locations of small (0.424- and 0.49-m-diam) orifices (unlike any of the others where good agreement was obtained).

Calculated and experimental temperatures are shown in Figs. A-60--64. The trend is the same as for previous experiments D9 and D11. Good agreement is obtained for R7, R6, and R8, which had stagnant volumes (Figs. A-60, A-63, and A-64), but the calculated temperature is much higher for those rooms (R5 and R4) with longitudinal flow (Figs. A-61, A-62).

F. Experiment D15

Calculated and experimental absolute pressures for R6, R8, R7, R4, and R9 are shown in Figs. A-65--69. As in the previous experiments, good agreement is obtained between measurement and calculation for the first 0.2 s, with an overprediction of pressure (~0.1-0.3 bar) near the end of blowdown (~2.5 s)

Calculated and experimental differential pressures are shown in Figs. A-70--73. Good agreement is obtained for the differential pressures between R6 and R4 (Fig. A-70), R8 and R4 (Fig. A-71), and R7 and R4 (Fig. A-72). The overall pressure differential, that is, between R6 and R9, is slightly over-predicted (Fig. A-73), but the agreement is still quite good.

Calculated and experimental temperature measurements for test D15 are shown in Figs. A-74--78. The obvious trend is that the calculated temperatures

are higher than measured, consistent with the comparisons shown for the other experiments for rooms with longitudinal flow.

G. Summary

The COMPARE MOD-1 application to the Battelle-Frankfurt D-series tests and comparisons with experimental data show the following.

- In general, the code predicts pressures that are higher than those measured for all subcompartments; the greatest overprediction occurs near the blowdown source with better agreement near the containment (sink) volume.
- In general, the predicted differential pressures at overflow cross sections are higher than those measured. Comparison of the results for experiments D1 and D6 show that better agreement for differential pressures is obtained across orifices than across nozzles.
- In general, the calculated temperatures are higher than those measured at locations in the flow stream. Good agreement is obtained at locations of low flow rates (dead-ends).
- Where jet effects are important (for example, experiment D9, R8), the difference between calculation and measurement is even greater than it is at other locations.

V. MOD-2 RESULTS FOR EXPERIMENT D1

A. Introduction

The MOD-2 version of COMPARE uses the method-of-characteristics (MOC) approach to solve the complete equations for the one-dimensional flow of an ideal gas in a constant area duct.[13,14] As a result, the effects of compressibility and density variations with length are automatically provided for. Two-dimensional effects are not provided for by the MOC approach, so we have used loss coefficients in conjunction with the compressible ideal gas nozzle equations to account for area changes caused by duct inlet and exit and to orifices or nozzles. The MOD-2 code requires at least one source and sink condition in the form of stagnant volumes at the duct ends for the definition of boundary conditions. Flows with water, steam, and air are assumed to be

homogeneous for the determination of properties that are used in the ideal gas and MOC equations.

B. Problem Formulation

The MOD-2 code was used to analyze the Battelle-Frankfurt D1 test, in which blowdown was introduced into one end of R6, left from the other end, and went to R4 through a nozzle. In R4, the flow proceeded upward and left through another nozzle going to R9, a large room (Fig. A-1).

Early attempts to use MOD-2 assumed that fractional parts of R6 near the break could accept the blowdown and establish an upstream stagnation source condition to be imposed on the MOC representation of the remainder of R6 and all of R4. R9 was the downstream stagnation volume. Unfortunately, severe pressure oscillations were calculated to occur in the blowdown volume. The imposition of these pressure variations on the MOC calculations caused numerical convergence problems. This problem was avoided by making all of R6 the blowdown volume.

C. Results

Two MOD-2 calculations for test D1 were performed: Run 1 used R6 as the blowdown volume, R4 as a MOC duct with nozzles at both ends, and R9 as a stagnant volume; run 2 was the same, except that the lower 25% of R4 was a stagnant volume, as in the MOD-1 calculations discussed above. This was done because the flow enters the lower part of R4 horizontally and must turn upward. Significant mixing probably would result and the assumption of a stagnation condition might be appropriate. Loss coefficient and geometric descriptions were the same as those used for the MOD-1 calculations.

Figures A-79 and A-80 show the measurements and the MOD-1 calculated results of both calculations. The pressures in R6 are compared in Fig. A-79 and R9 pressures are compared in Fig. A-80. The MOD-2 calculations compare favorably with the measurements, with maximum R6 pressures within about 10% of the measurements. An interesting result is that the MOD-2 calculation predicts R9 pressures below the measurements, which is expected if upstream calculated pressures are higher than measured, as at early times. This expectancy is based on the conservation of mass and energy principle and on pressure increasing with increasing mass and energy. Note that this does not happen with the MOD-1 calculation.

One explanation for the difference between the MOD-2 and MOD-1 results is the difference between entry and exit mass flow rates in R4, as shown in Fig. A-81. The MOD-2 results indicate that considerably more mass is stored in R4, which would explain the lower MOD-2 R9 pressure.

D. Summary and Conclusions

The MOD-2 code application and the comparison of the MOD-2 and MOD-1 calculated and test results show that

- MOD-2 MOC approach calculations compare well with the measurements;
- MOD-2 calculations compare better with the measurements than the MOD-1 code;
- MOD-2 requires a better means for representing the blowdown boundary condition than the stagnation volume approach currently available;
- the tests are still difficult to model because certain effects, such as jets, are not conveniently modeled; and
- blowdown room pressures and the blowdown room-to-sink pressure differences are calculated to be greater than those measured.

VI. PARAMETER STUDIES AND RELATED WORK

A. Previous Studies with COMPARE

The main purpose of this study is to present a comparison of COMPARE predicted results with experimental results using regulatory assumptions. The calculated and measured data comparisons allow a determination of the degree of conservatism exhibited in the calculated results. We have not attempted to adjust code parameters to obtain good fit to the experimental data, nor have we performed a best-estimate calculation.

However, for design of verification experiments or to perform best-estimate calculations, it is important to know how sensitive these results are to both the initial and boundary conditions and to parameters contained within the code. The sensitivity of the code predictions to variations in its parameters has already been studied in detail in Ref. 3, which presents the sensitivity of calculated results to the following code parameters:

- subcompartment nodalization,
- use of the Homogeneous Equilibrium Model rather than the Moody critical flow model,

- Moody Multiplier correction factor, and
- liquid entrainment effects.

However, we conclude that, in general, a reasonable variation in these parameters will not bring the calculations in line with the experimental measurements. Therefore, additional parameters and effects must be investigated to produce a good best-estimate calculation.

The possibility of using other codes for the calculations has also been explored. As mentioned in Sec. III, experiment D15 formed the basis for an international Containment Analysis Standard Problem. COMPARE MOD-1 calculations were performed for this experiment before January 1978 without knowledge of the experimental results, except for the provided mass and energy release data. In addition, at least 11 sets of calculations from different codes were submitted by others. The detailed results of all these calculations are compared against experimental data in Ref. 15.

It is not appropriate to compare the various code results with each other because some calculations were performed with regulatory subcompartment analysis assumptions and others were performed with best-estimate assumptions: for example, the inclusion of heat sinks. However, in general, COMPARE results compare quite favorably with results of similar codes and models. The best comparisons with the measured pressures were obtained using more sophisticated codes such as BEACON.[16] The best temperature predictions were made by codes that model heat transfer effects, which appear to be important (discussed below) in the D-series tests. Heat transfer effects were not modeled in the results presented here.

B. Sensitivity to Blowdown Fluid Quality

We have shown that the COMPARE MOD-1 calculations tend to predict temperatures and presssures higher than measured for nearly all time and space points in the D-series experiments. From the equation of state, we conclude that we are overpredicting either the mass of fluid in the system or the energy stored in the fluid. Because the initial conditions are known and the blowdown mass flow rate is specified, it appears that we are overpredicting the total system internal energy. This could be caused by either of two effects; (1) overprediction of the blowdown fluid enthalpy, or (2) neglecting heat transfer from the fluid to the containment walls. In this section we

discuss the sensitivity of the first effect. The second will be discussed in Sec. E.

The intent of the D-series tests was to use saturated steam as the blowdown fluid. Because the blowdown source is some distance (~30 m) from the containment, the actual blowdown fluid may be slightly wet rather than saturated steam. We have performed a calculation for experiment D1 to investigate the sensitivity of the calculated results to this parameter.

Figure A-82 shows the effect of the blowdown fluid quality on the temperature in R4. The base case run (100% quality) is the same calculation as shown in Fig. A-13. Notice that a drop of only 5% quality in the blowdown fluid leads to a noticeable improvement in the R4 temperature calculation. Figure A-83 shows the R4 pressure results for the same set of calculations. Again, decrease of quality of the blowdown fluid leads to a much better code prediction.

The results of this calculation are not presented to cast doubts on the experimental measurements, but the calculations do show that an error in the blowdown fluid enthalpy is a plausible explanation for part of the difference between experiment and measurement in the computed results. Furthermore, it shows that this is an important experimental input and accurate measurement could be crucial to good code predictions.

C. Sensitivity to Inertia

A concern in previous similar analyses was the importance of the inclusion of the inertia effect and its effect on the calculational results. Experiment D1 was selected as a basis for a parametric study of the sensitivity of the calculated results to the value of inertia included in the calculation. The experiment was simulated with COMPARE using the noding shown in Fig. A-1. For the base case calculation, the calculational parameters used were those shown in Tables I and VI. Two additional calculations were performed; the first used values for inertia one-half of those shown in Table VI, and the second used values double those shown in Table VI. None of the other parameters was altered.

The results of the three calculations are shown in Table XVIII. The table compares the maximum calculated differential pressure between the three rooms and the time at which this maximum pressure differential occurred. The results indicate that the sensitivity of these two parameters to the value of inertia is small.

TABLE XVIII

COMPARE CALCULATED MAXIMUM DIFFERENTIAL PRESSURES AND THEIR TIME OF OCCURRENCE FOR THREE DIFFERENT VALUES OF INERTIA FOR EXPERIMENT D1

Relative value of inertia	Volumes 3-4/5 ΔP (bars)	Volumes 3-4/5 Time (s)	Volumes 4-6/7 ΔP (bars)	Volumes 4-6/7 Time (s)	Volumes 6-8/9 ΔP (bars)	Volumes 6-8/9 Time (s)
1/2[a]	0.337	0.30	0.464	0.32	0.759	1.45
1	0.326	0.24	0.467	0.29	0.746	1.42
2[b]	0.341	0.25	0.496	0.47	1.004	1.44

[a] This calculation used 1/2 the values of inertia shown in Table I.

[b] This calculation used twice the values of inertia shown in Table I.

[c] The volumes indicated are those shown in Fig. 1.

TABLE XIX

COMPARE CALCULATED MAXIMUM DIFFERENTIAL PRESSURES AND THEIR TIME OF OCCURRENCE FOR THREE DIFFERENT NODING SCHEMES FOR EXPERIMENT D1

Model	Total No. of Nodes	R6/R4 Junction ΔP (bars)	R6/R4 Junction Time (s)	R4/R9 Junction ΔP (bars)	R4/R9 Junction Time (s)
1	3	0.29	0.27	0.45	0.41
2[a]	10	0.33	0.28	0.45	0.43
3	19	0.34	0.26	0.46	0.43

[a] Model 2 is the base case calculation shown in Fig. 1. The results are slightly different from those shown in Table XVIII, inertia x 1, because wall friction is not included in this calculation.

D. Sensitivity to Noding

A concern in analyses such as those presented here is whether a sufficient number of nodes has been used in the computer model simulating the physical geometry. Experiment D1 was selected as a basis for a parametric study of the sensitivity of the calculated results as a function of the number of nodes selected in the computer model. Three different noding configurations were investigated.

1. Three nodes total. R6, R4, and R9 each represent one volume in the COMPARE model.
2. Ten nodes total. Five nodes in R6, 4 nodes in R4, and 1 node in R9. This noding scheme is shown in Fig. A-1, and is identical to the noding used in the previous calculations shown above for COMPARE MOD-1.
3. Nineteen nodes total. Ten nodes in R6, 8 nodes in R4, and 1 node in R9. This noding basically consists of doubling (over the base case) the number of nodes in R6 and R4.

To allow a direct comparison of results for the three cases, no attempt was made to include wall friction in the entrance and exit losses for the junctions.

The results of the three calculations are shown in Table XIX. The table compares the maximum calculated differential pressure across the two nozzles and the time at which this maximum pressure differential occurred. The results show that increasing the number of nodes from 3 to 10 changes the maximum differential pressure appreciably, but increasing the number of nodes from

10 to 19 alters the results only slightly. We expect that if more nodes were used, the results would be unchanged. Futhermore, this study indicates that a sufficient number of nodes were used in the base case calculations discussed in Sec. IV. of this report. There is reasonable assurance that the main results of this report would be valid if the computer simulation of the experiments were rerun with an increased number of nodes in the model.

E. Summary of Parameter Studies Performed by Others

Overprediction of temperature and pressure in computer code calculations of these experiments has been typical in many calculations.[7--12] This has generated a significant amount of effort to determine which code parameters could be adjusted to obtain good best-estimate calculations. Most of these studies have been conducted by Gesellschaft fur Reaktorsicherheit (GRS) and focus mainly on the heat transfer between the containment walls and containment atmosphere. The codes used, COFLOW and ZOCO 6, are similar to COMPARE, so their results probably will apply to COMPARE calculations as well.

The results of the calculations of experiment D1 using COFLOW[17] show that the computer predictions of both temperature and pressure are greatly improved by using a heat transfer coefficient of approximately 10^4 W/m^2K between the containment walls and atmosphere. The calculations also show that results of using the Tagami[18] heat transfer correlation are not much better than the base case (no heat transfer).

Reference 8 shows a similar trend for experiment D6, in which the calculation used a heat transfer coefficient of 1300 W/m^2K. In general, lower pressurization was exhibited (compared with the base case) but there was still an overprediction of pressure in the rupture subcompartment. However, the temperature calculations are greatly improved.

Similar calculations for experiment D9 using ZOCO 6 are reported in Ref. 19. Heat transfer coefficients of approximately 3000 W/m^2K were used to produce good results. Similar results and assumptions are presented in Ref. 10 for experiment D11 and in Ref. 11 for experiment D14.

The results of these parametric studies indicate that using a large value of the heat transfer coefficient with high velocity flows yields much better code predictions of both temperature and presssure. Therefore, it appears that heat transfer within the containment is an important parameter to study for best-estimate calculations. However, as stated in Ref. 11, it is generally

thought that the magnitude of the coefficients used in these studies were unrealistically large in comparison with conventional containment condensing heat transfer correlations. As a result, it is recommended that other physical phenomena be investigated.

On the other hand, we believe that the existence of higher-than- conventional coefficients should not be rejected, primarily because the physics of the D-series tests were much different from those for the tests that form the basis for the conventional correlations. In particular, the conventional correlations[18,20] are for large air-fraction volumes without a directed flow. By contrast, not only is directed flow common in the D-series tests, but it might move most of the air ahead of the blowdown. As a result, it seems that certain areas experienced high heat transfer rates because of the condensation of relatively pure steam with some velocity.

VII. CONCLUSIONS AND RECOMMENDATIONS

A. Conclusions

COMPARE MOD-1 results (using regulatory assumptions) obtained here are conservative in the sense that

- in general, the subcompartment pressures are overpredicted;
- in general, the overflow cross-section differential pressures are overpredicted; and
- in general, the subcompartment temperatures are overpredicted.

As expected, the pressure predictions are less accurate where the geometric complexity of the experiment precludes code modeling of important effects (for example, jet effects).

COMPARE MOD-2 results indicate that some conservatism in the MOD-1 calculations may be due to treatment of one-dimensional effects. The MOD-2 predictions are more accurate in the pressure calculation than those of MOD-1. This may be because the codes predict significantly different mass flow rates between compartments. Unfortunately, there are no experimental flow rate measurements to compare against the calculated results.

Many parametric studies have been performed using COMPARE and other codes to quantify the sensitivity of the computed results to various models and input

data to the codes. Two parameters that could explain much of the conservatism in the calculations are (1) the enthalpy of the blowdown fluid, and (2) containment atmosphere to wall and condensation heat transfer. The selection of best-estimate values for these parameters has not been addressed in this report. Because critical flow did not occur in either the experiment or calculations, the Battelle-Frankfurt D-series tests do not allow a detailed analysis of the adequacy of the critical flow models incorporated in COMPARE.

A review of the CASP results for experiment D15 shows that COMPARE MOD-1 results, in general, compare quite favorably to those produced by similar codes. It may be possible to obtain much better results using advanced codes such as BEACON.

B. Recommendations

It is reassuring to report that, for this series of tests, calculated results from COMPARE MOD-1 are conservative in the sense that the absolute pressures, differential pressures, and temperatures are overpredicted. However, the reasons for the conservatism are not entirely understood. We feel that the nature of the conservatism involved could be best understood by performing a best-estimate calculation for one experiment and evaluating the relative importance of the different effects.

Three principal code models contained in COMPARE MOD-1 that should be investigated are the compressible flow, heat transfer, and geometric models.

- The validity of the flow prediction models used in the code should be assessed with respect to their predictive ability when applied to water-steam-air mixtures.
- The relative importance of heat transfer effects in the D-series tests should be assessed. One of the experiments should be recalculated using a reasonable value for the condensation heat transfer coefficient. The parameter studies performed by others should be studied to assess the validity of the magnitude of the heat transfer coefficient used to produce the best-estimate results.
- The importance of the effects of complex system geometry should be assessed. This includes jet effects, corners and constrictions, which are not modeled adequately in COMPARE.

The above objectives could be accomplished most efficiently by a comparison of COMPARE results with those obtained by a best-estimate advanced code that produces results that agree closely with the experimental data. Note that comparisons between the BEACON and COMPARE codes and the Battelle-Frankfurt data are scheduled to be performed in FY 1980. We must use other analytical predictions rather than the experimental data because the crucial parameters, the heat transfer and mass flow rates, are not measured. If a code produces good comparisons with pressure and temperature measurements, it is assumed that predictions are good for unmeasured quantities (if they are important). COMPARE results are similar for all the D-series tests, so comparison would only be necessary for one of the simpler tests rather than the whole series. The relatively simple geometries of D1 and D6 make them likely candidates for this comparison.

The data provided by this set of experiments were valuable in assessing the predictive capabilities of COMPARE; however, they would have been much more valuable with error bands on the data and with mass flow rate data at the orifices, and we recommend that future experiments include such measurements.

Reference 3 presents a detailed proposal for a feasibility study to see if it is possible to create an experiment that can isolate parameters that affect analytical predictions. We recommend, as a result of our experience, that such a feasibility study be initiated.

REFERENCES

1. "Standard Review Plan for the Review of Safety Analysis Reports for Nuclear Power Plants," Section 6.2.1.2. Office of Nuclear Reactor Regulation, US Nuclear Regulatory Commission report NUREG-0800, LWR edition, formerly NUREG-75/087.

2. R. G. Gido, J. S. Gilbert, R. G. Lawton, and W. L. Jensen, "COMPARE MOD-1: A Code for the Transient Analysis of Volumes With Heat Sinks, Flowing Vents, and Doors," Los Alamos Scientific Laboratory report LA-7199-MS (March 1978).

3. W. S. Gregory, J. R. Campbell, R. G. Gido, and A. J. Webb, "Comparison of COMPARE/RELAP-3 Subcompartment Calculations With Battelle-Frankfurt C-Series Test Results," Los Alamos Scientific Laboratory report to be published.

4. "Investigation of the Phenomena Occurring Within a Multi-Compartment Containment After Rupture of the Primary Cooling Circuit in Water-Cooled Reactors," US Nuclear Regulatory Commission report NUREG/TR-0043 (November 1977).

5. T. F. Kanzleiter, "Experimental Investigations of Pressure and Temperature Loads on a Containment After a Loss-of-Coolant Accident," Nuclear Engineering Design 38, pp. 159-167 (March 1976).

6. I. E. Idelichik, "Handbook of Hydraulic Resistance, Coefficients of Local Resistance and of Friction," US Department of Commerce report AEC-6630 (1966).

7. "Investigation of the Phenomena Occurring Within a Multi-Compartment Containment After Rupture of the Primary Cooling Circuit in Water-Cooled Reactors," Battelle-Institute e.V. Frankfurt/Main West Germany, Technischer Bericht BF-RS50-32-D1 (May 1977).

8. "Investigation of the Phenomena Occurring Within a Multi-Compartment Containment After Rupture of the Primary Cooling Circuit in Water-Cooled Reactors," Battelle-Institute e.V. Frankfurt/Main West Germany, Technischer Bericht BF-RS50-32-D6 (May 1977).

9. Investigation of the Phenomena Occurring Within a Multi-Compartment Containment After Rupture of the Primary Cooling Circuit in Water-Cooled Reactors," Battelle-Institute e.V. Frankfurt/Main West Germany, Technischer Bericht BF-RS50-32-D9 (November 1977).

10. "Investigation of the Phenomena Occurring Within a Multi-Compartment Containment After Rupture of the Primary Cooling Circuit in Water-Cooled Reactors," Battelle-Institute e.V. Frankfurt/Main West Germany, Technischer Bericht BF-RS50-32-D11 (January 1978).

11. "Investigation of the Phenomena Occurring Within a Multi-Compartment Containment After Rupture of the Primary Cooling Circuit in Water-Cooled Reactors," Battelle-Institute e.V. Frankfurt/Main West Germany, Technischer Bericht BF-RS50-32-D14 (June 1978).

12. "Investigation of the Phenomena Occurring Within a Multi-Compartment Containment After Rupture of the Primary Cooling Circuit in Water-Cooled Reactors," Battelle-Institute e.V. Frankfurt/Main West Germany, Technischer Bericht BF-RS50-32-D15-2 (November 1978).

13. M. J. Zucrow and J. D. Hoffman, Gas Dynamics, Vols. 1 and 2 (John Wiley and Sons, New York, 1977).

14. A. H. Shapiro, The Dynamics and Thermodynamics of Compressible Fluid Flow, Vols. 1 and 2 (Ronald Press, New York, 1953).

15. W. Winkler, "Deutsches Standard-Problem No. 1, Dampfleitungsbruch in einer Raumkette," Gesellschaft fur Reaktorsicherheit (GRS)(February 1979).

16. R. A. Wells, "BEACON/MOD2A: A Computer Program for Subcompartment Analysis of Nuclear Reactor Containment--User's Manual," EG&G Idaho, Inc. report CDAP-TR-051 (March 1979).

17. G. Hellings, "Nachrechnungen zu den beim Battelle-Institute, Frankfurt/Main Durchgefuhrten versuchen D1 und D3 des RS 50 Forschungsvorhabens Druckverteilung in Containment," Gesellschaft fur Reaktorsicherheit (GRS) report GRS-A-72 (December 1977).

18. T. Tagami, "Interim Report on Safety Assessments and Facilities Establishment Project in Japan for Period Ending June 1965 (No. 1)," unpublished work, February 28, 1966.

19. "Investigation of the Phenomena Occurring Within a Multi-Compartment Containment After Rupture of the Primary Cooling Circuit in Water-Cooled Reactors," US Nuclear Regulatory Commission report NUREG/TR-0043 (November 1977).

20. H. Uchida, A. Oyama, and T. Togo, "Evaluation of Post Incident Cooling Systems of Light-Water Power Reactors," in Proceedings of the Third International Conference on the Peaceful Uses of Atomic Energy Held in Geneva, August 31, 1964, Volume 13, New York: United Nations, 1965 (A/Conf. 28/10/436) (May 1964).

APPENDIX

COMPARISON OF COMPARE MOD-1 SUBCOMPARTMENT CALCULATIONS
WITH BATTELLE-FRANKFURT D-SERIES TEST RESULTS

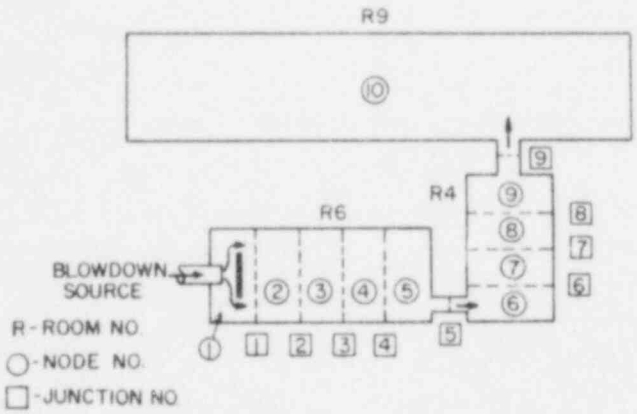

Fig. A-1. Experimental configuration and COMPARE noding for experiments D1 and D6.

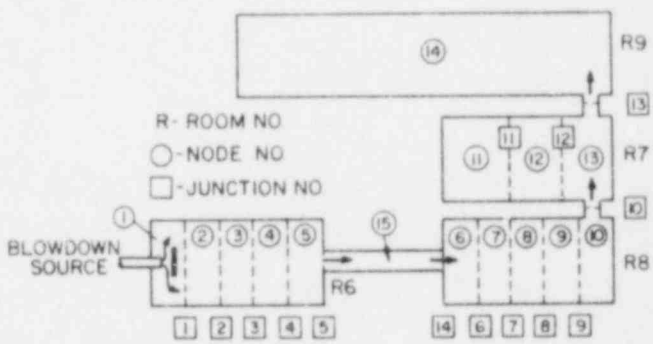

Fig. A-2. Experimental configuration and COMPARE noding for experiment D9.

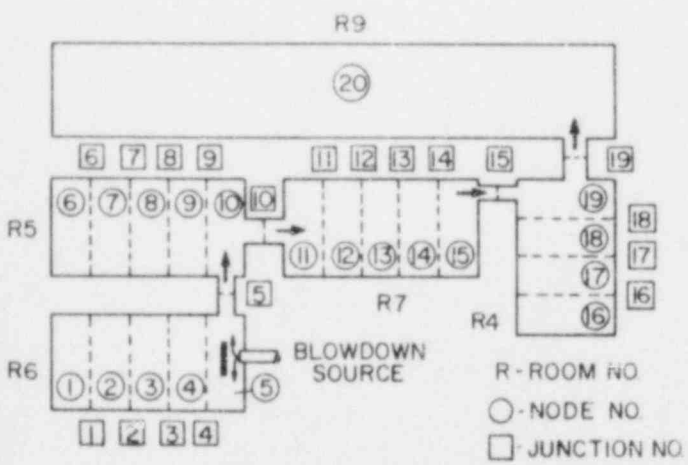

Fig. A-3. Experimental configuration and COMPARE noding for experiment D11.

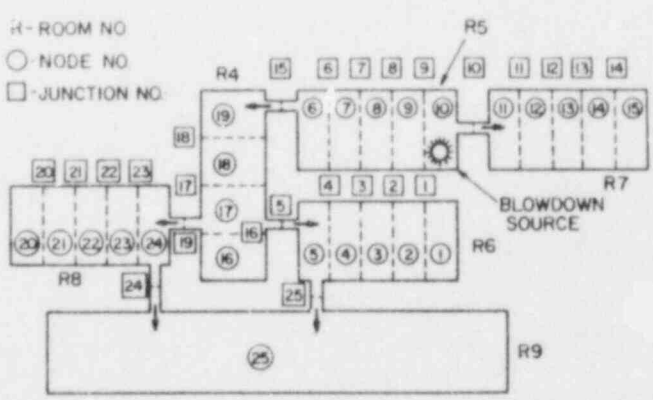

Fig. A-4. Experimental configuration and COMPARE noding for experiment D14.

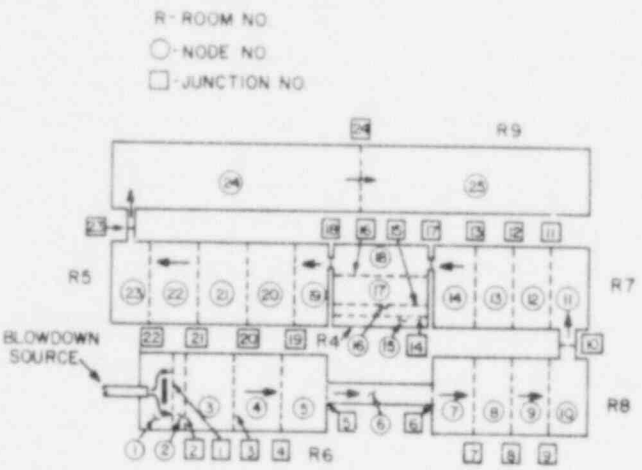

Fig. A-5. Experimental configuration and COMPARE noding for experiment D15.

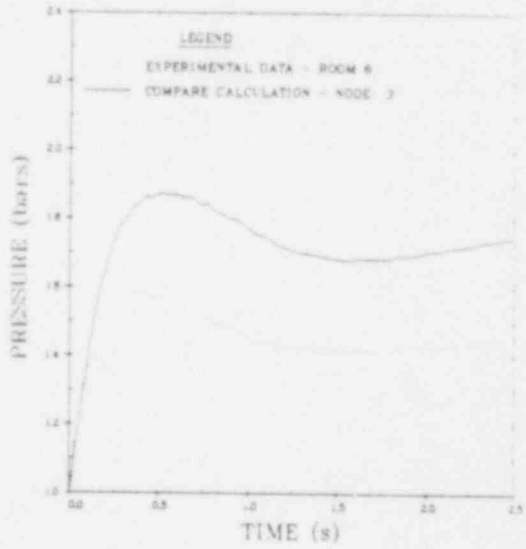

Fig. A-6. Comparison of COMPARE MOD-calculation with experimental data for test D1, room 6 pressure.

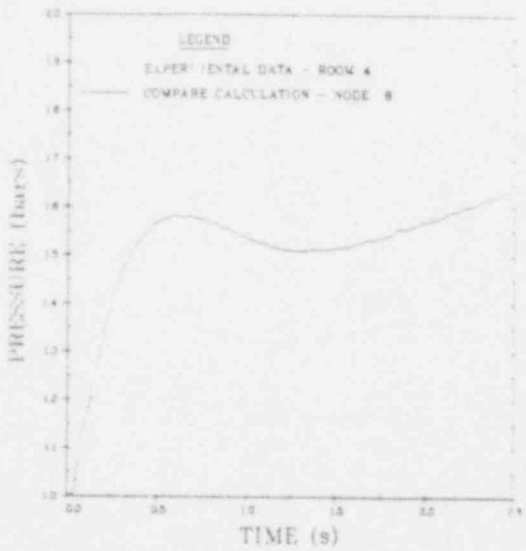

Fig. A-7. Comparison of COMPARE MOD-1 calculation with experimental data for test D1, room 4 pressure.

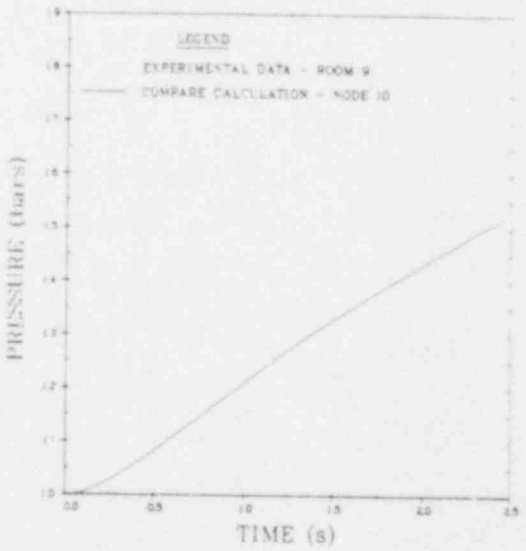

Fig. A-8. Comparison of COMPARE MOD-1 calculation with experimental data for test D1, room 9 pressure.

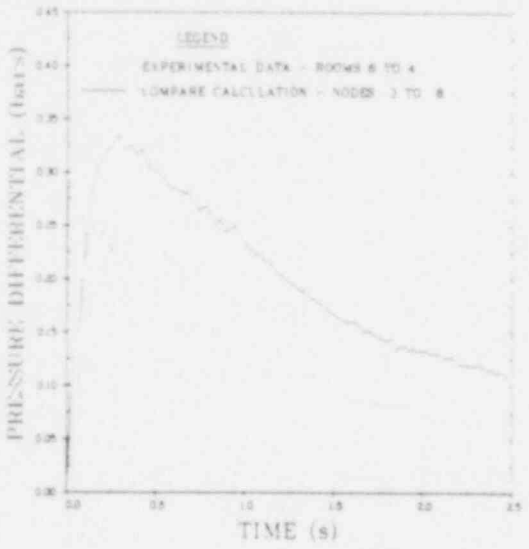

Fig. A-9. Comparison of COMPARE MOD-1 calculation with experimental data for test D1, room 6 to room 4 differential pressure.

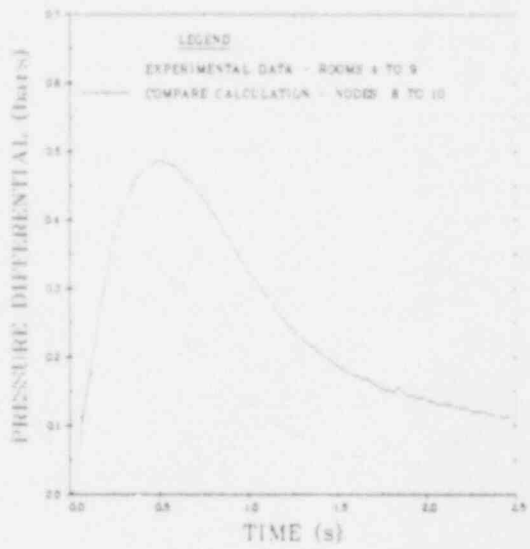

Fig. A-10. Comparison of COMPARE MOD-1 calculation with experimental data for test D1, room 4 to room 9 differential pressure.

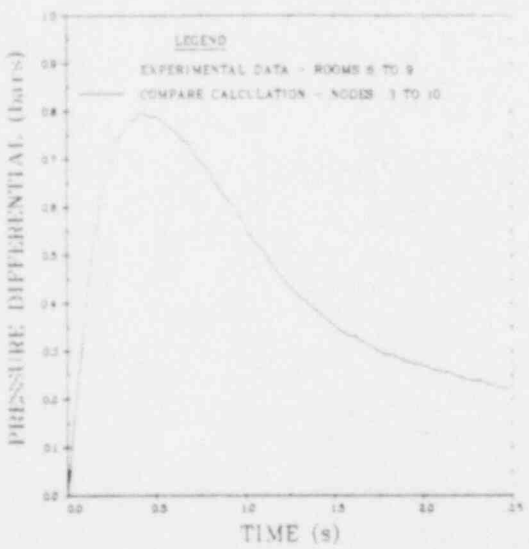

Fig. A-11. Comparison of COMPARE MOD-1 calculation with experimental data for test D1, room 6 to room 9 differential pressure.

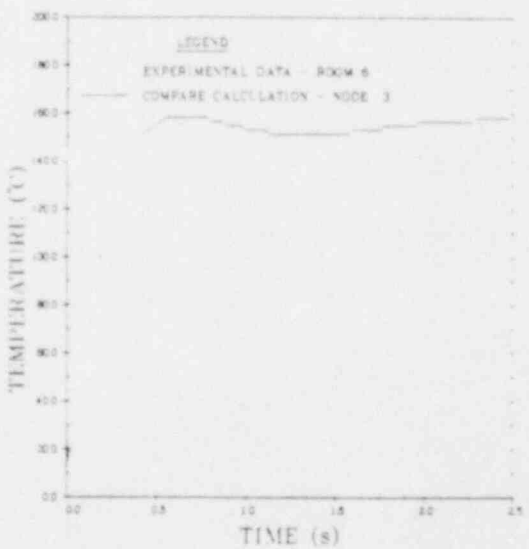

Fig. A-12. Comparison of COMPARE MOD-1 calculation with experimental data for test D1, room 6 temperature.

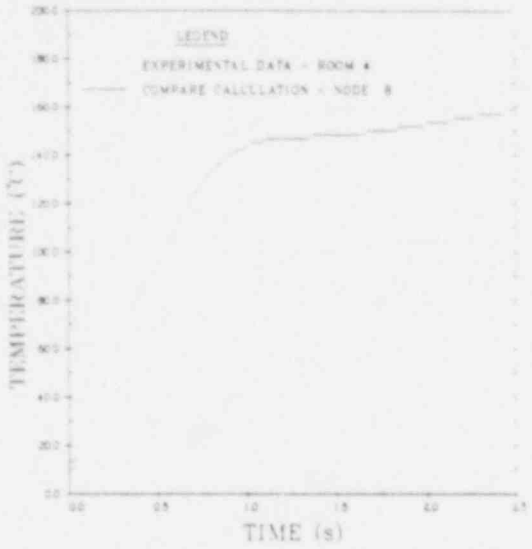

Fig. A-13. Comparison of COMPARE MOD-1 calculation with experimental data for test D1, room 4 temperature.

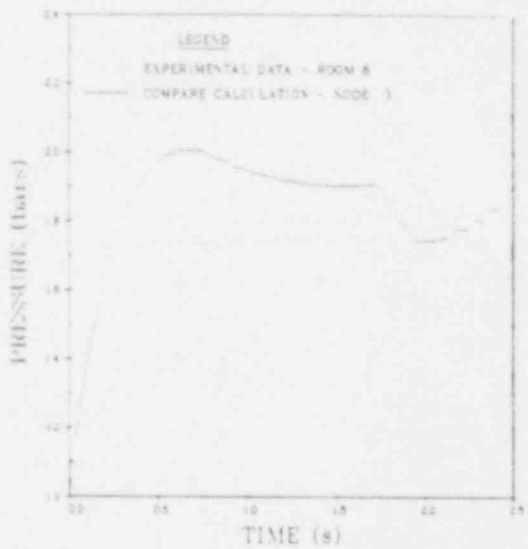

Fig. A-14. Comparison of COMPARE MOD-1 calculation with experimental data for test D6, room 6 pressure.

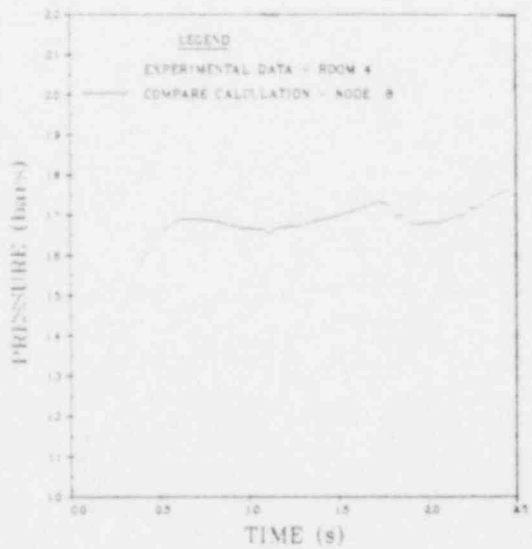

Fig. A-15. Comparison of COMPARE MOD-1 calculation with experimental data for test D6, room 4 pressure.

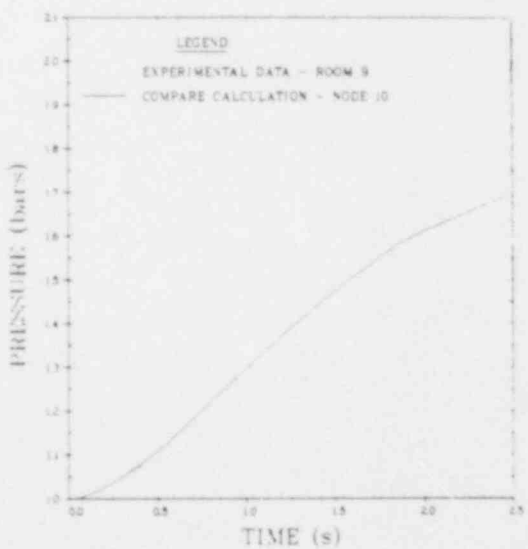

Fig. A-16. Comparison of COMPARE MOD-1 calculation with experimental data for test D6, room 9 pressure.

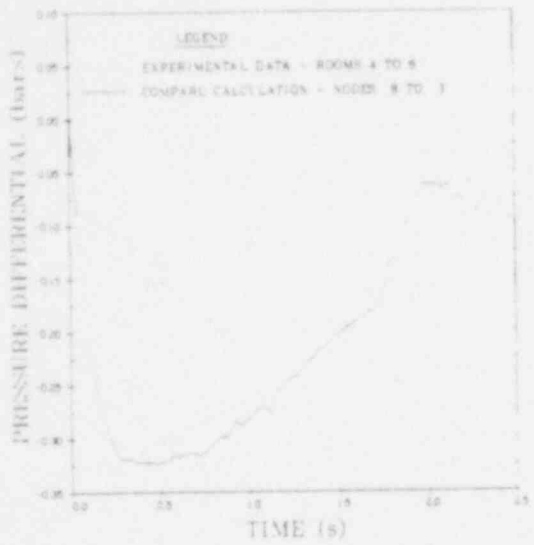

Fig. A-17. Comparison of COMPARE MOD-1 calculation with experimental data for test D6, room 6 to room 4 differential pressure.

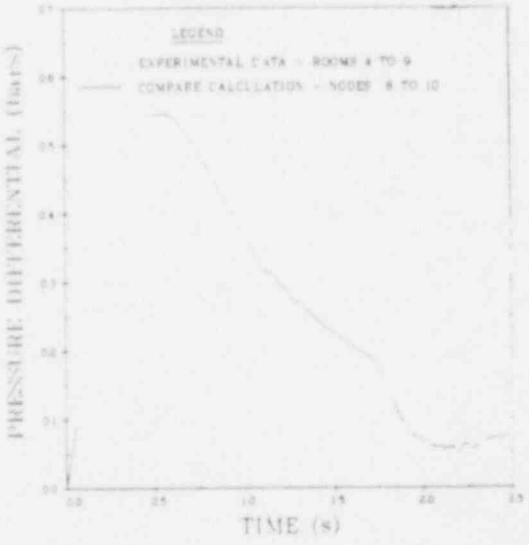

Fig. A-18. Comparison of COMPARE MOD-1 calculation with experimental data for test D6, room 4 to room 9 differential pressure.

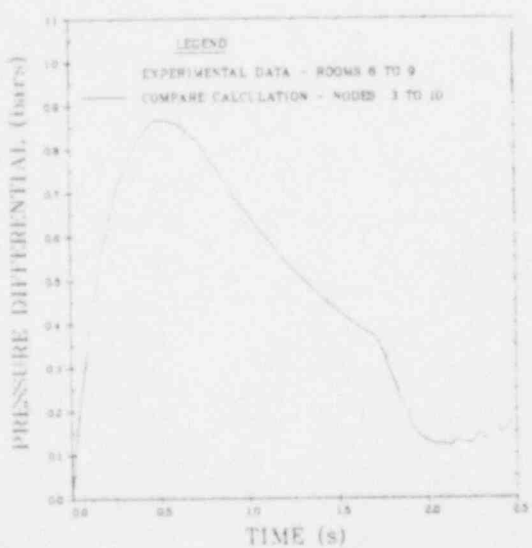

Fig. A-19. Comparison of COMPARE MOD-1 calculation with experimental data for test D6, room 6 to room 9 differential pressure.

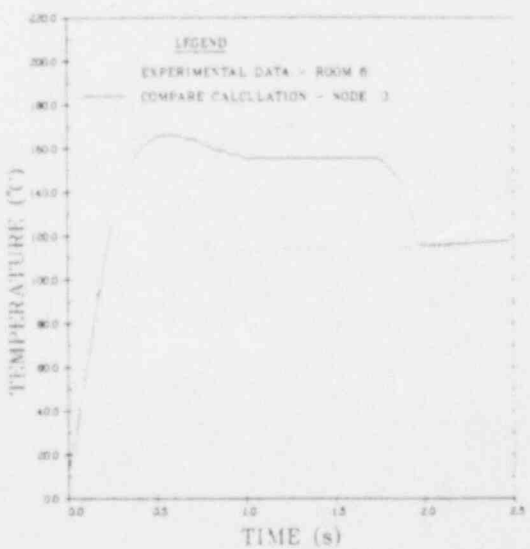

Fig. A-20. Comparison of COMPARE MOD-1 calculation with experimental data for test D6, room 6 temperature.

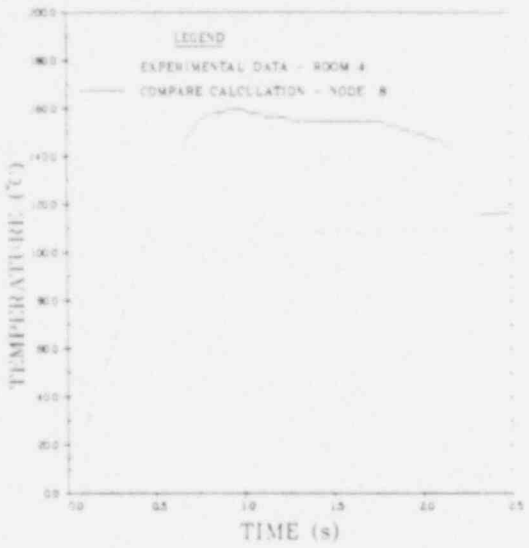

Fig. A-21. Comparison of COMPARE MOD-1 calculation with experimental data for test D6, room 4 temperature.

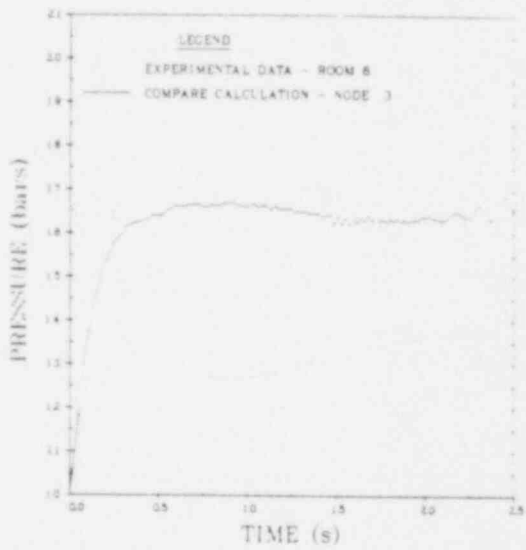

Fig. A-22. Comparison of COMPARE MOD-1 calculation with experimental data for test D9, room 6 pressure.

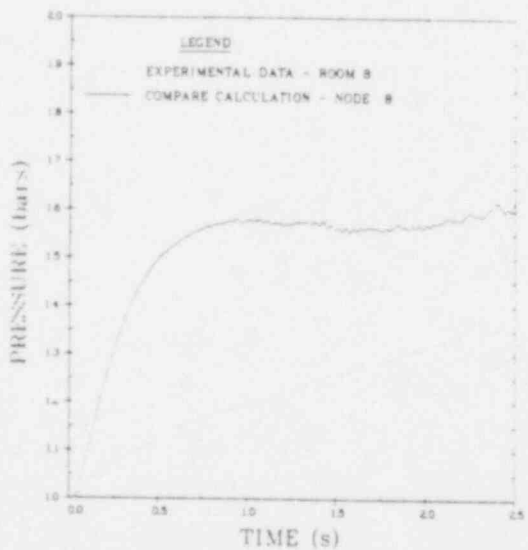

Fig. A-23. Comparison of COMPARE MOD-1 calculation with experimental data for test D9, room 8 pressure.

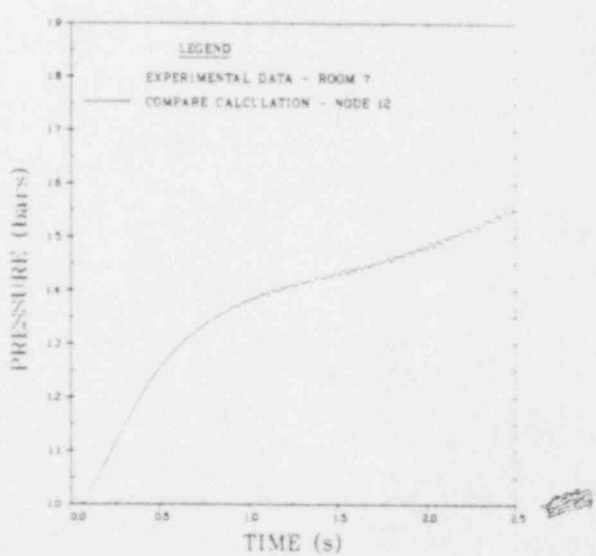

Fig. A-24. Comparison of COMPARE MOD-1 calculation with experimental data for test D9, room 7 pressure.

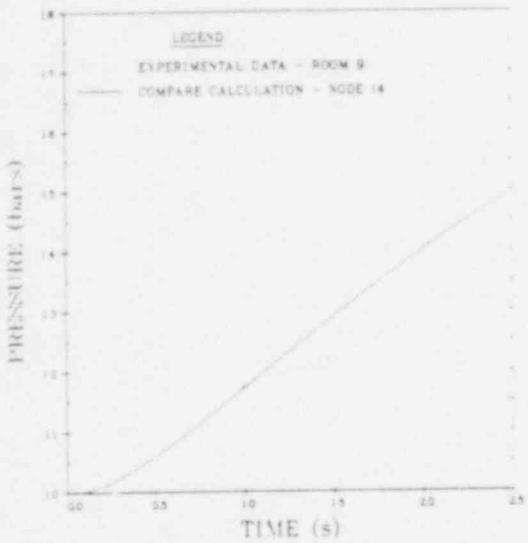

Fig. A-25. Comparison of COMPARE MOD-1 calculation with experimental data for test D9, room 9 pressure.

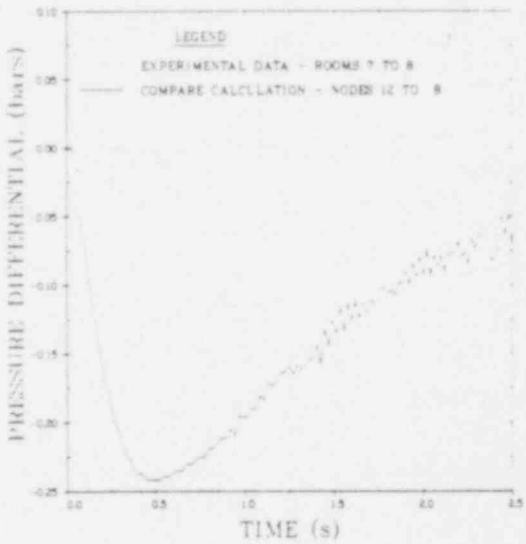

Fig. A-26. Comparison of COMPARE MOD-1 calculation with experimental data for test D9, room 7 to room 8 differential pressure.

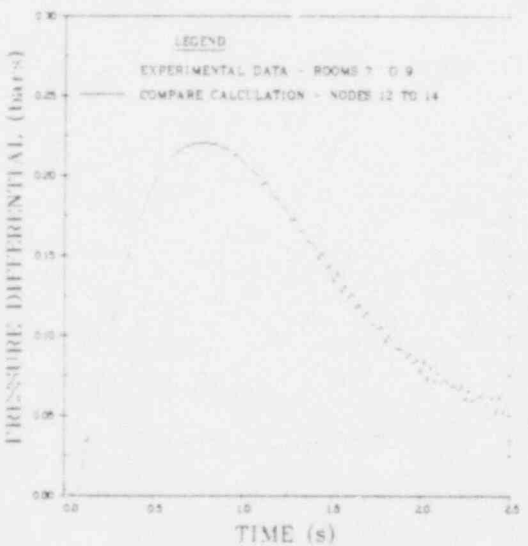

Fig. A-27. Comparison of COMPARE MOD-1 calculation with experimental data for test D9, room 7 to room 9 differential pressure.

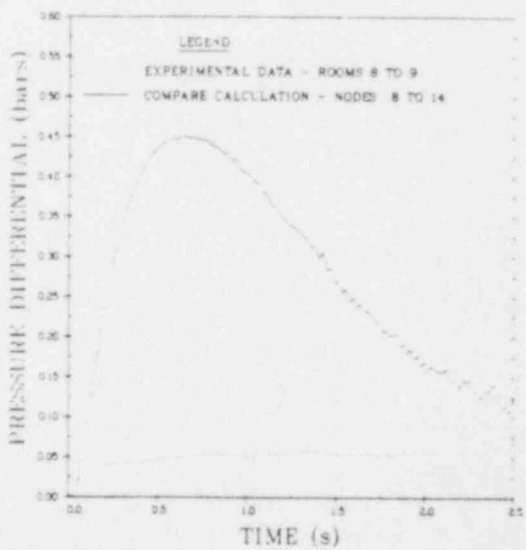

Fig. A-28. Comparison of COMPARE MOD-1 calculation with experimental data for test D9, room 8 to room 9 differential pressure.

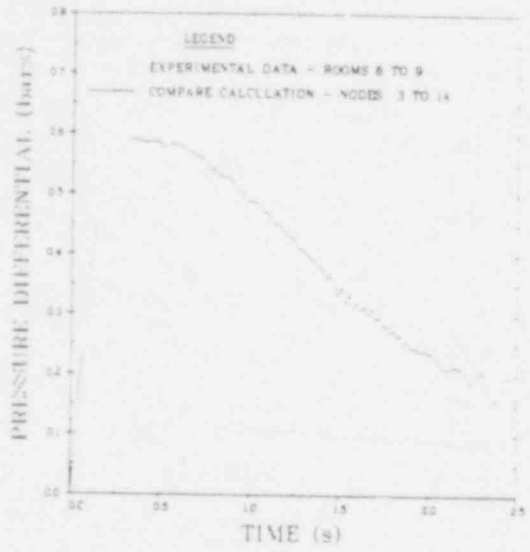

Fig. A-29. Comparison of COMPARE MOD-1 calculation with experimental data for test D9, room 6 to room 9 differential pressure.

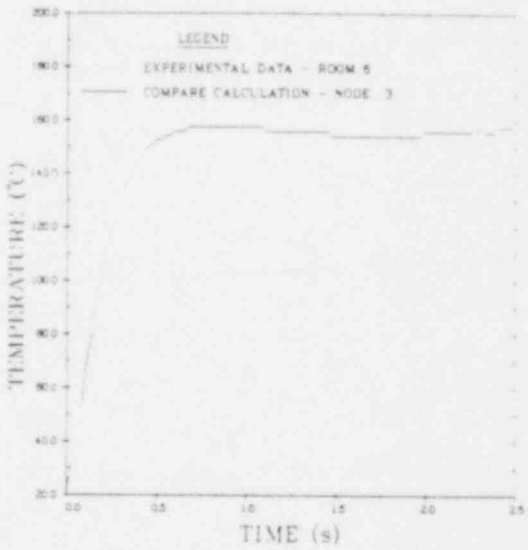

Fig. A-30. Comparison of COMPARE MOD-1 calculation with experimental data for test D9, room 6 temperature.

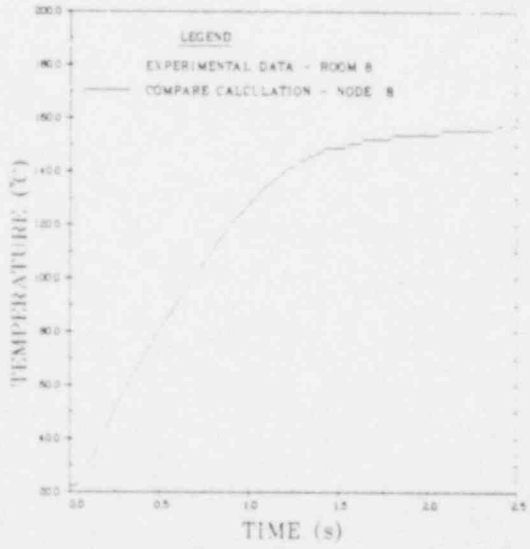

Fig. A-31. Comparison of COMPARE MOD-1 calculation with experimental data for test D9, room 8 temperature.

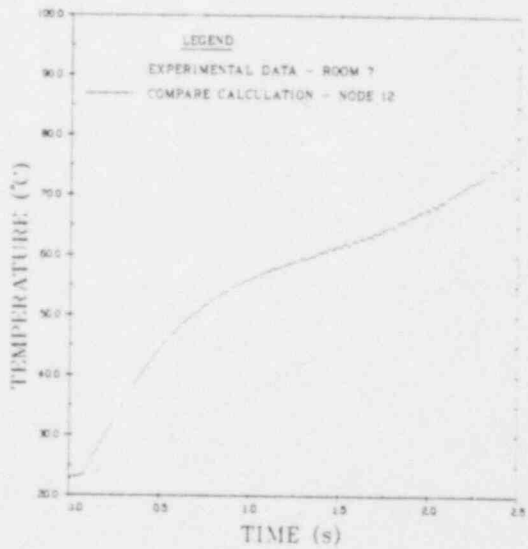

Fig. A-32. Comparison of COMPARE MOD-1 calculation with experimental data for test D9, room 7 temperature.

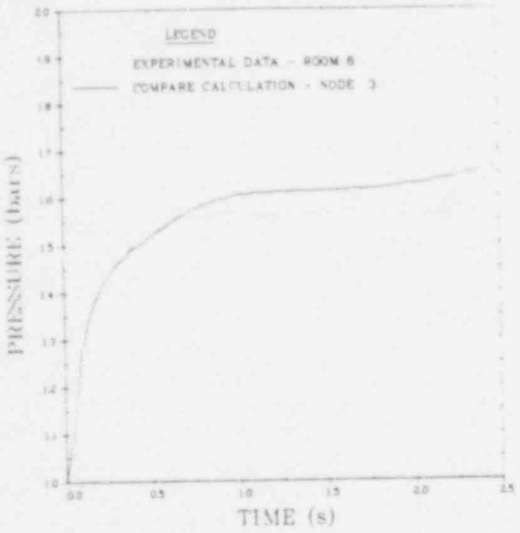

Fig. A-33. Comparison of COMPARE MOD-1 calculation with experimental data for test D11, room 6 pressure.

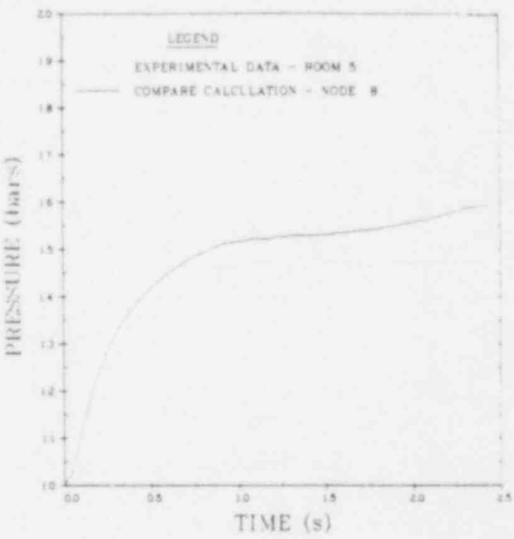

Fig. A-34. Comparison of COMPARE MOD-1 calculation with experimental data for test D11, room 5 pressure.

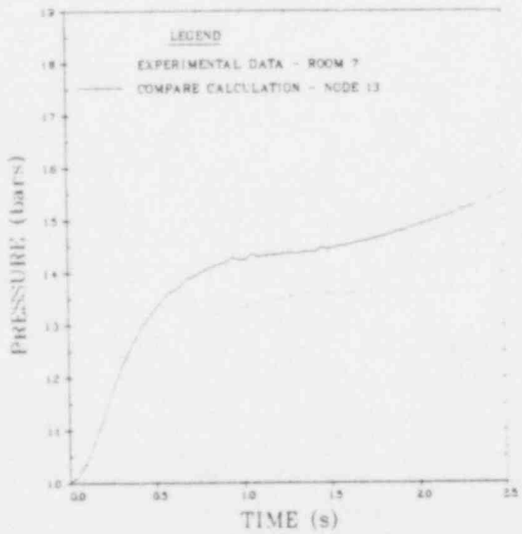

Fig. A-35. Comparison of COMPARE MOD-1 calculation with experimental data for test D11, room 7 pressure.

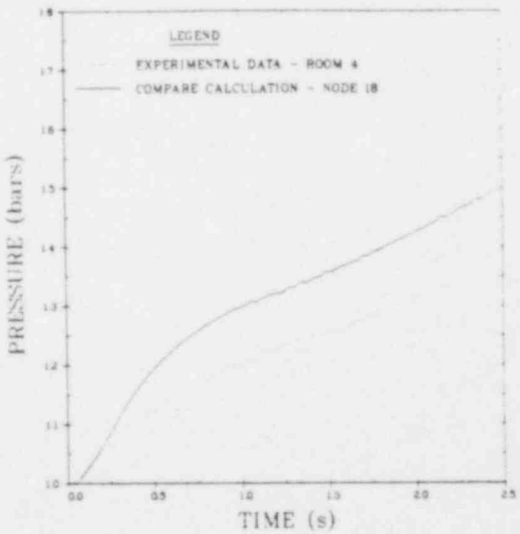

Fig. A-36. Comparison of COMPARE MOD-1 calculation with experimental data for test D11, room 4 pressure.

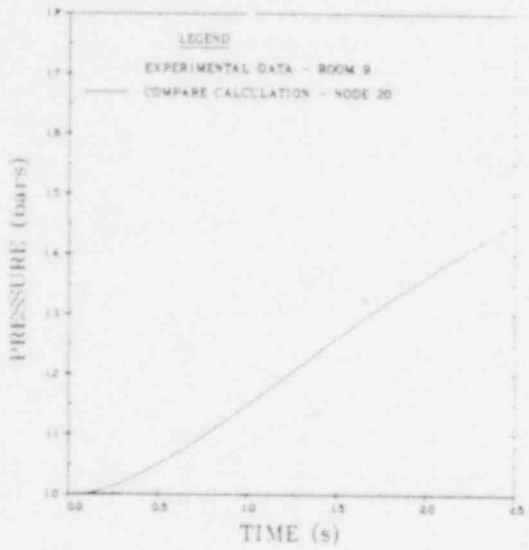

Fig. A-37. Comparison of COMPARE MOD-1 calculation with experimental data for test D11, room 9 pressure.

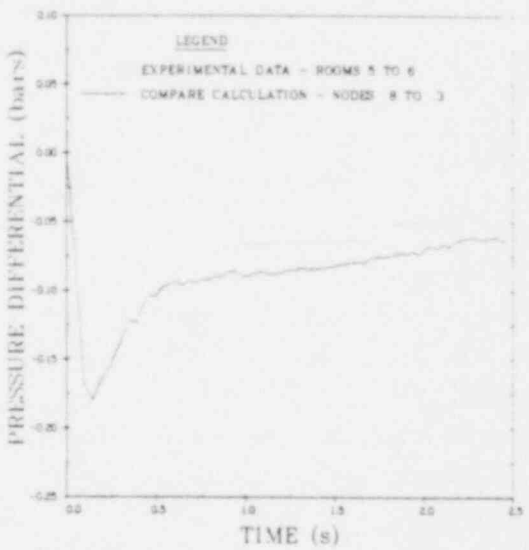

Fig. A-38. Comparison of COMPARE MOD-1 calculation with experimental data for test D11, room 5 to room 6 differential pressure.

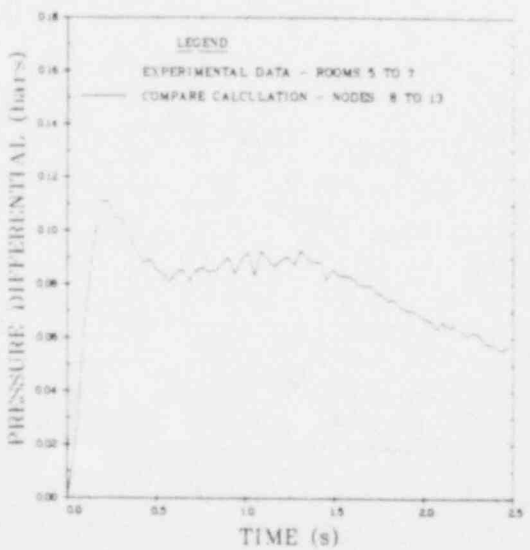

Fig. A-39. Comparison of COMPARE MOD-1 calculation with experimental data for test D11, room 5 to room 7 differential pressure.

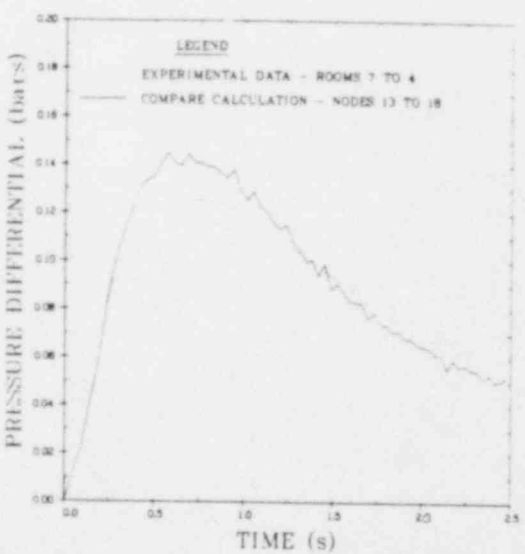

Fig. A-40. Comparison of COMPARE MOD-1 calculation with experimental data for test D11, room 7 to room 4 differential pressure.

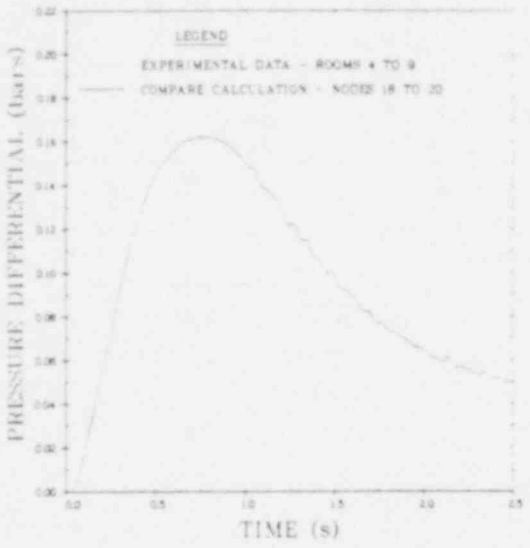

Fig. A-41. Comparison of COMPARE MOD-1 calculation with experimental data for test D11, room 4 to room 9 differential pressure.

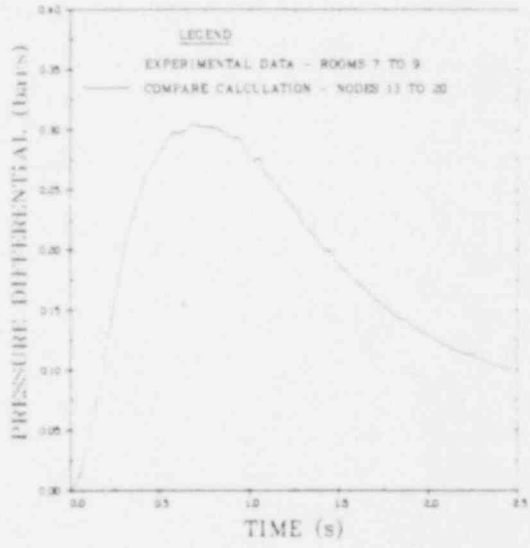

Fig. A-42. Comparison of COMPARE MOD-1 calculation with experimental data for test D11, room 7 to room 9 differential pressure.

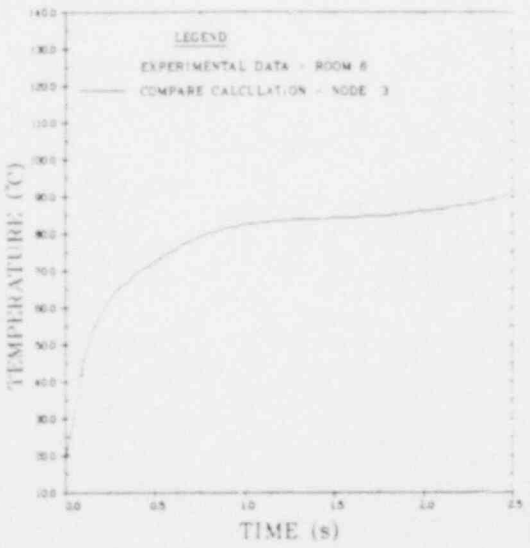

Fig. A-43. Comparison of COMPARE MOD-1 calculation with experimental data for test D11, room 6 temperature.

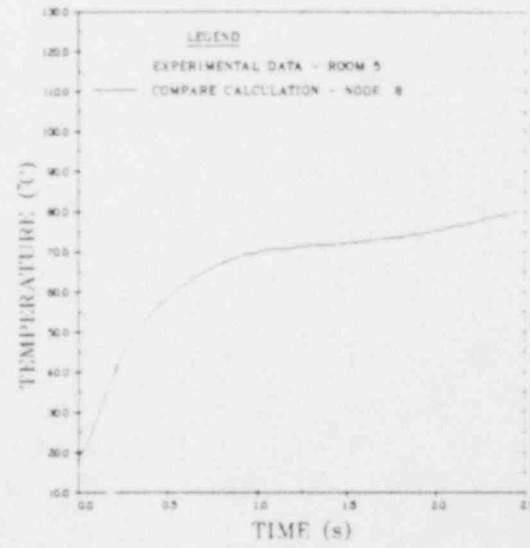

Fig. A-44. Comparison of COMPARE MOD-1 calculation with experimental data for test D11, room 5 temperature.

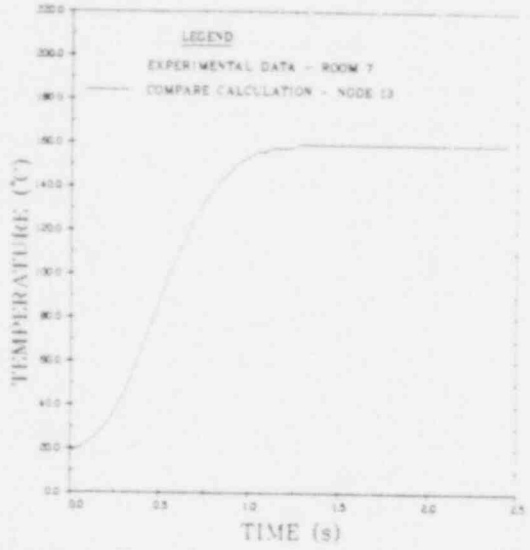

Fig. A-45. Comparison of COMPARE MOD-1 calculation with experimental data for test D11, room 7 temperature.

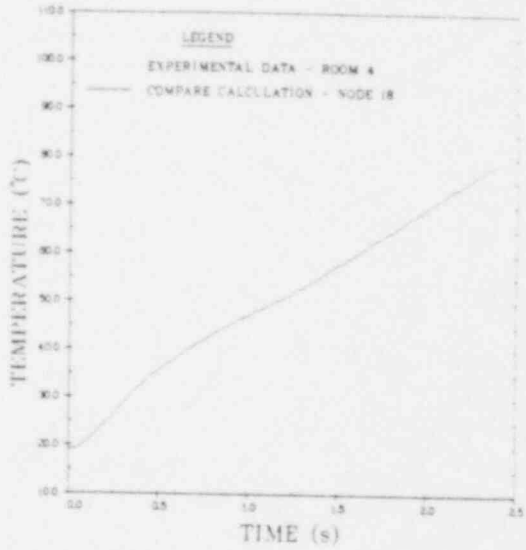

Fig. A-46. Comparison of COMPARE MOD-1 calculation with experimental data for test D11, room 4 temperature.

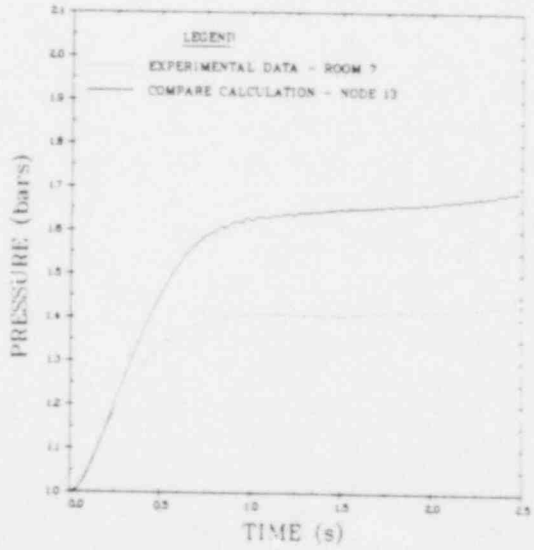

Fig. A-47. Comparison of COMPARE MOD-1 calculation with experimental data for test D14, room 7 pressure.

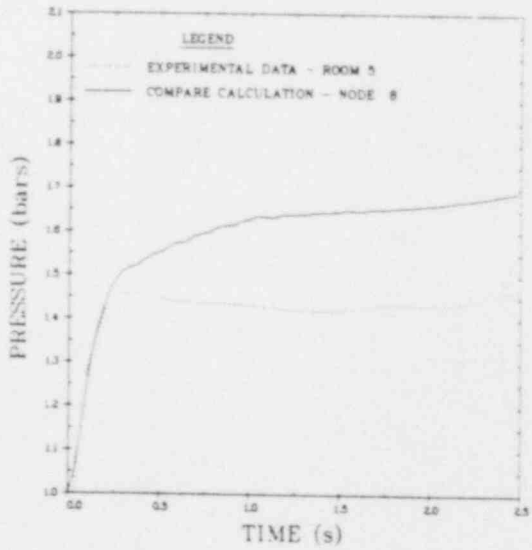

Fig. A-48. Comparison of COMPARE MOD-1 calculation with experimental data for test D14, room 5 pressure.

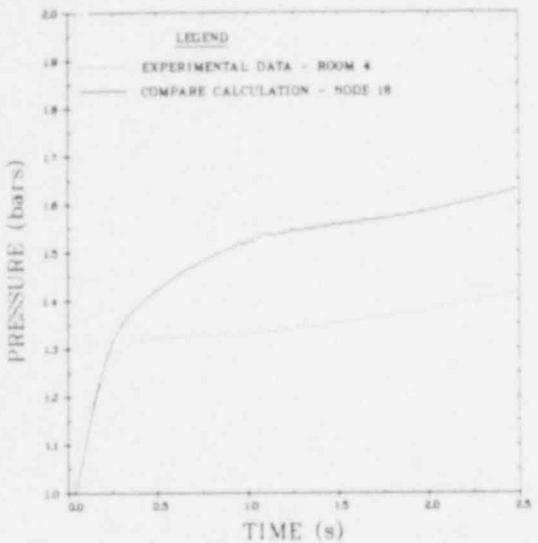

Fig. A-49. Comparison of COMPARE MOD-1 calculation with experimental data for test D14, room 4 pressure.

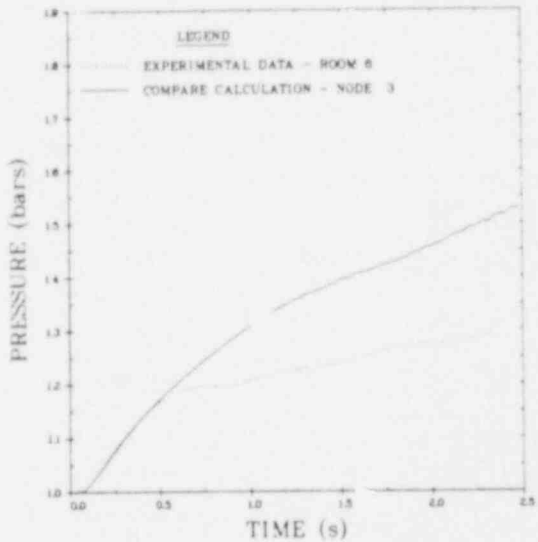

Fig. A-50. Comparison of COMPARE MOD-1 calculation with experimental data for test D14, room 6 pressure.

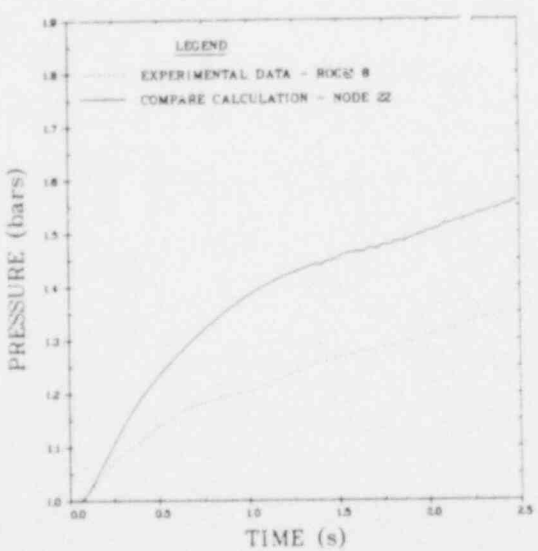

Fig. A-51. Comparison of COMPARE MOD-1 calculation with experimental data for test D14, room 8 pressure.

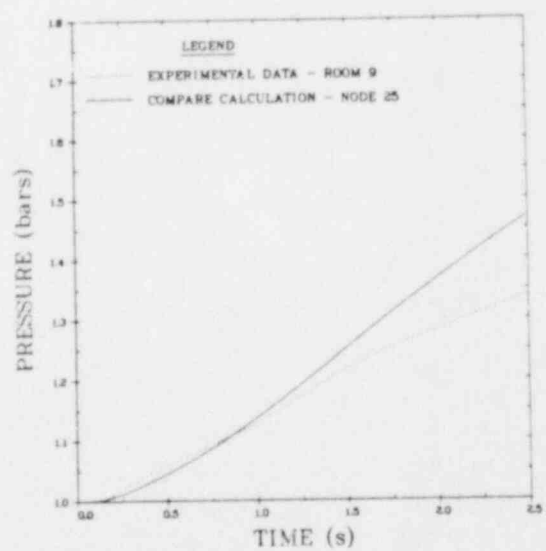

Fig. A-52. Comparison of COMPARE MOD-1 calculation with experimental data for test D14, room 9 pressure.

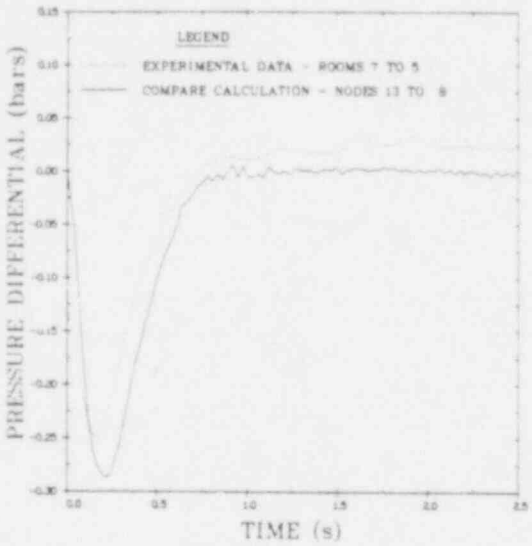

Fig. A-53. Comparison of COMPARE MOD-1 calculation with experimental data for test D14, room 7 to room 5 differential pressure.

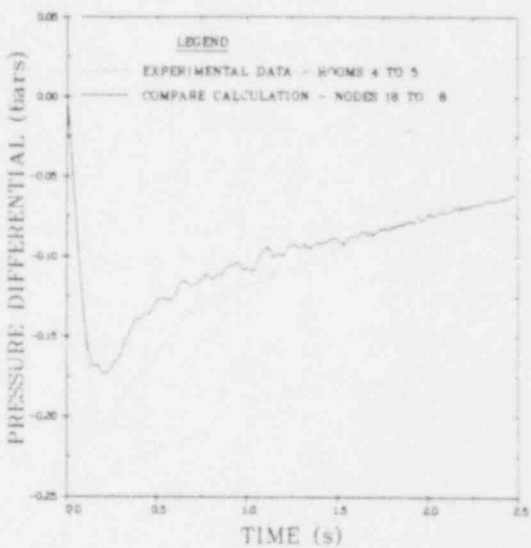

Fig. A-54. Comparison of COMPARE MOD-1 calculation with experimental data for test D14, room 4 to room 5 differential pressure.

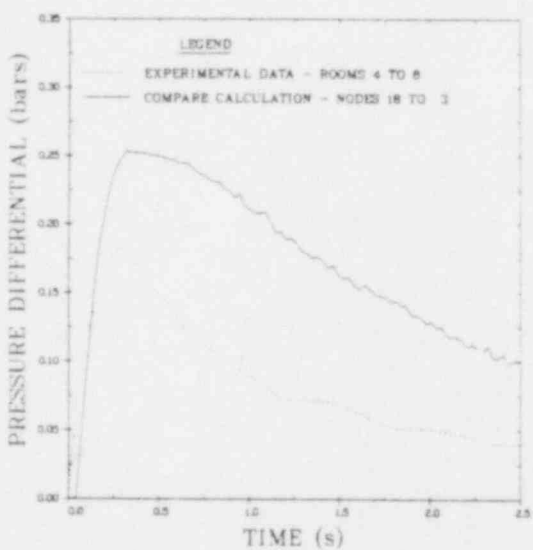

Fig. A-55. Comparison of COMPARE MOD-1 calculation with experimental data for test D14, room 4 to room 6 differential pressure.

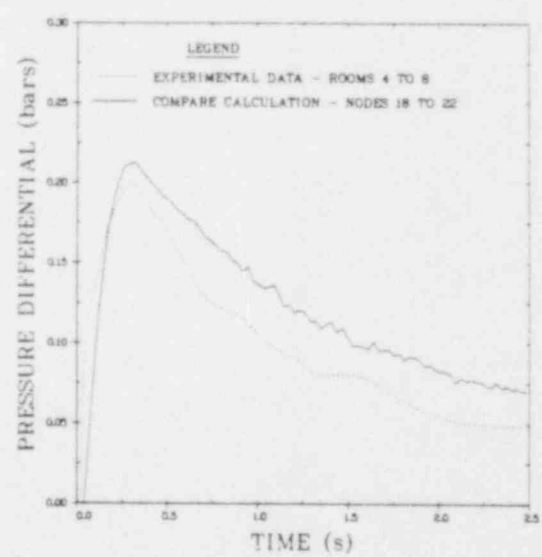

Fig. A-56. Comparison of COMPARE MOD-1 calculation with experimental data for test D14, room 4 to room 8 differential pressure.

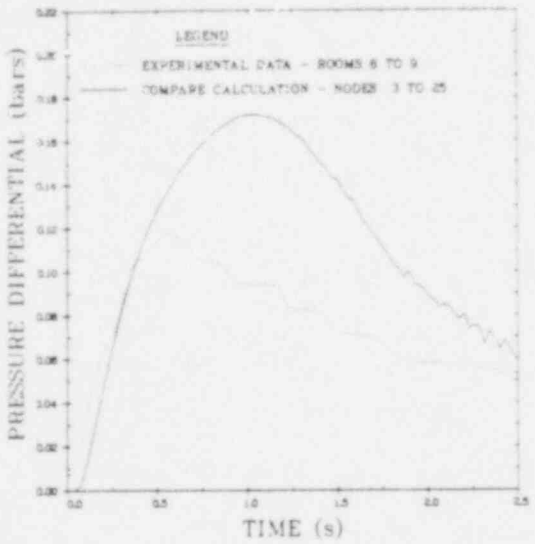

Fig. A-57. Comparison of COMPARE MOD-1 calculation with experimental data for test D14, room 6 to room 9 differential pressure.

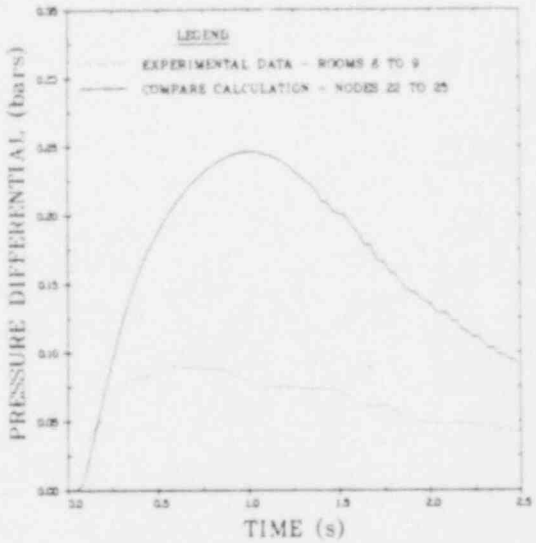

Fig. A-58. Comparison of COMPARE MOD-1 calculation with experimental data for test D14, room 8 to room 9 differential pressure.

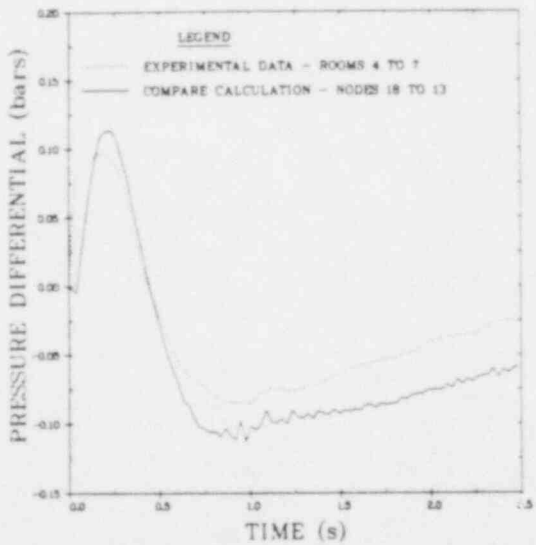

Fig. A-59. Comparison of COMPARE MOD-1 calculation with experimental data for test D14, room 4 to room 7 differential pressure.

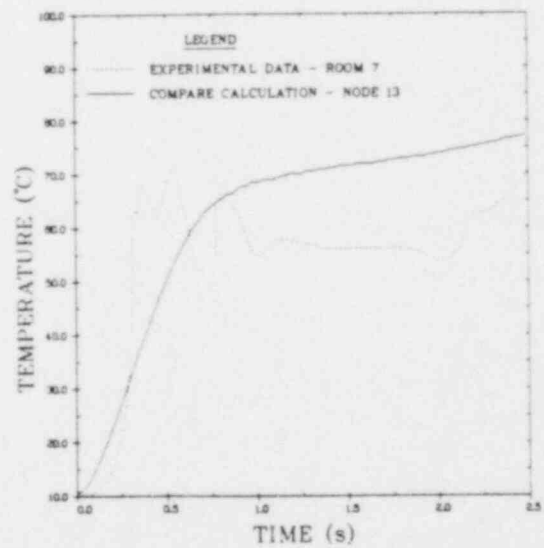

Fig. A-60. Comparison of COMPARE MOD-1 calculation with experimental data for test D14, room 7 temperature.

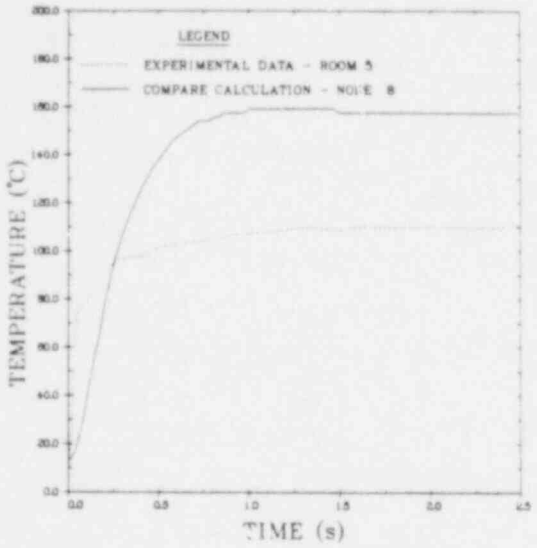

Fig. A-61. Comparison of COMPARE MOD-1 calculation with experimental data for test D14, room 5 temperature.

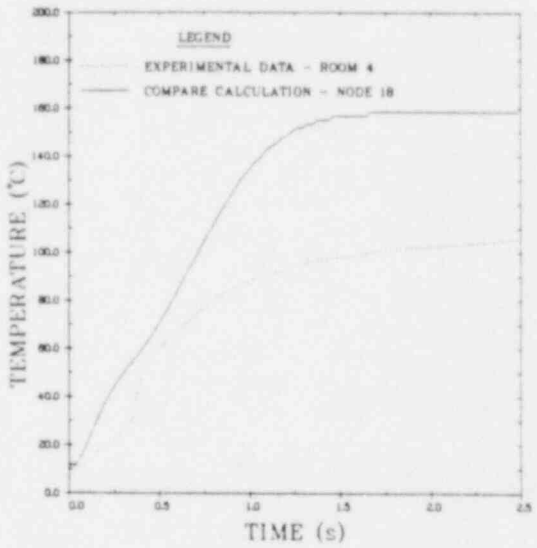

Fig. A-62. Comparison of COMPARE MOD-1 calculation with experimental data for test D14, room 4 temperature.

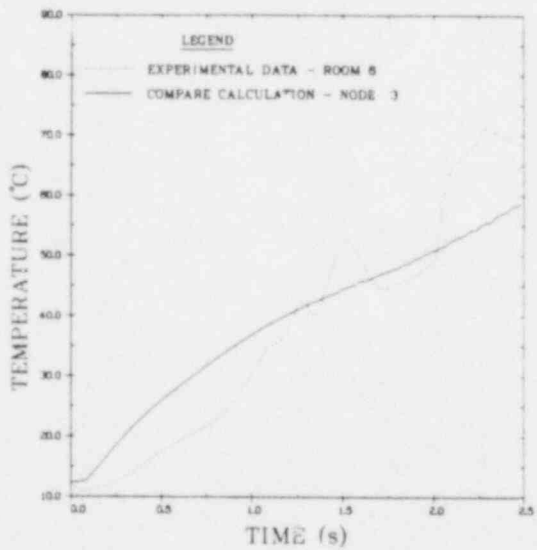

Fig. A-63. Comparison of COMPARE MOD-1 calculation with experimental data for test D14, room 6 temperature.

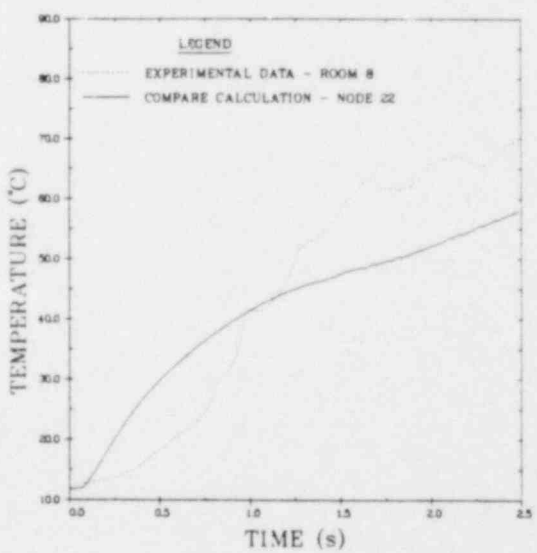

Fig. A-64. Comparison of COMPARE MOD-1 calculation with experimental data for test D14, room 8 temperature.

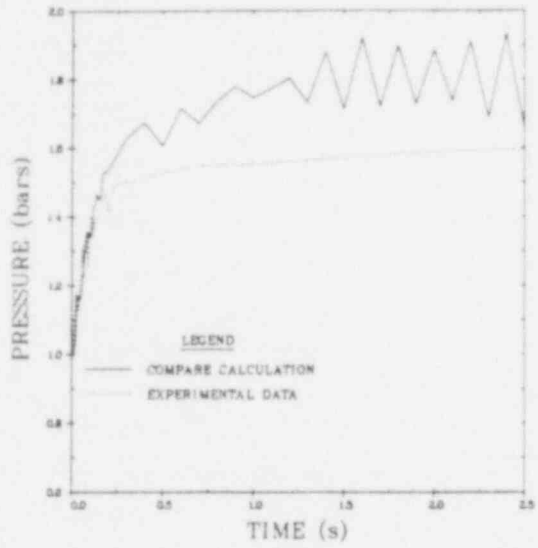

Fig. A-65. Comparison of COMPARE MOD-1 calculation with experimental data for test D15, room 6 pressure.

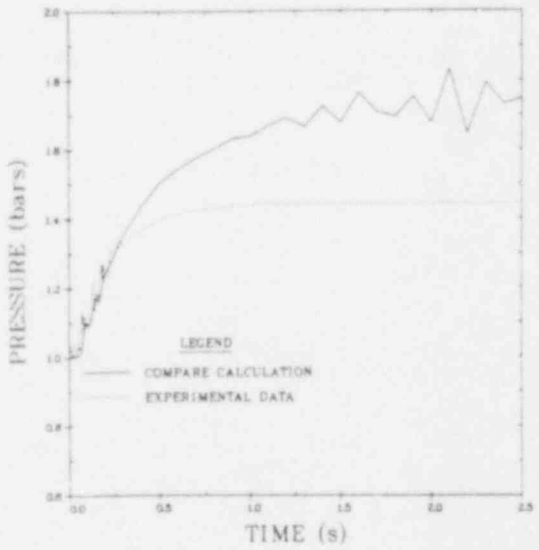

Fig. A-66. Comparison of COMPARE MOD-1 calculation with experimental data for test D15, room 8 pressure.

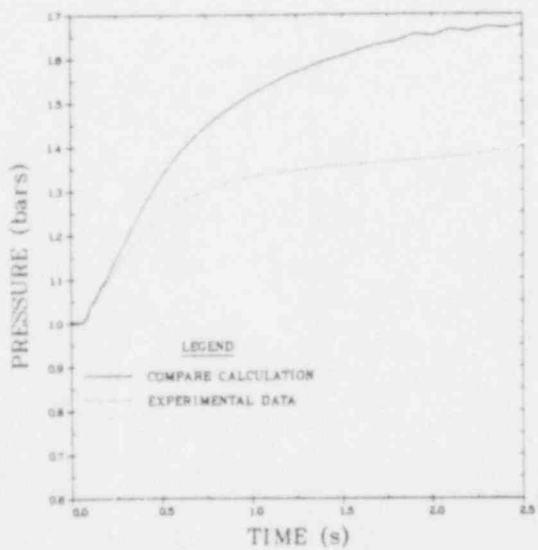

Fig. A-67. Comparison of COMPARE MOD-1 calculation with experimental data for test D15, room 7 pressure.

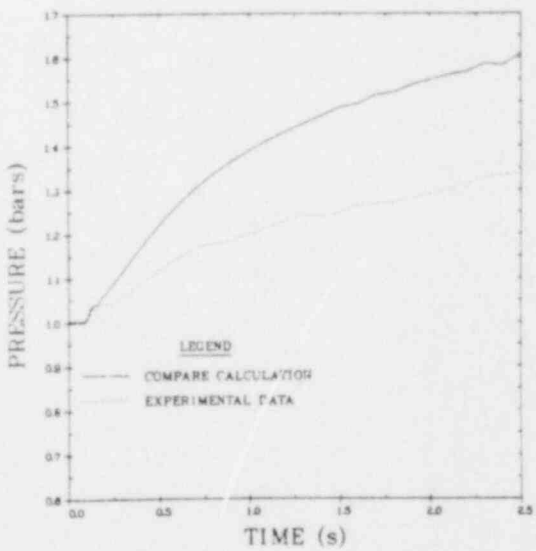

Fig. A-68. Comparison of COMPARE MOD-1 calculation with experimental data for test D15, room 4 pressure.

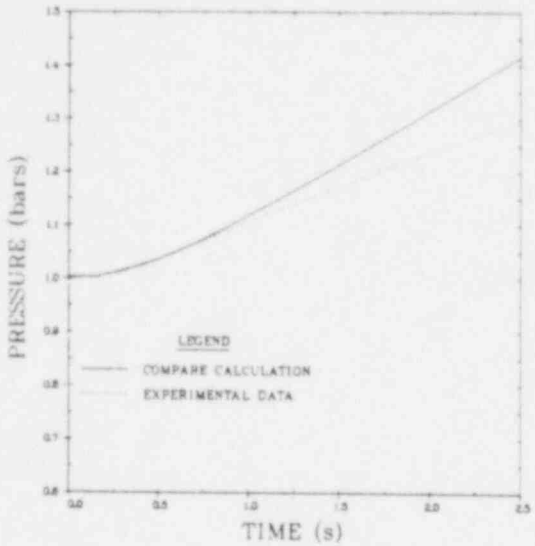

Fig. A-69. Comparison of COMPARE MOD-1 calculation with experimental data for test D15, room 9 pressure.

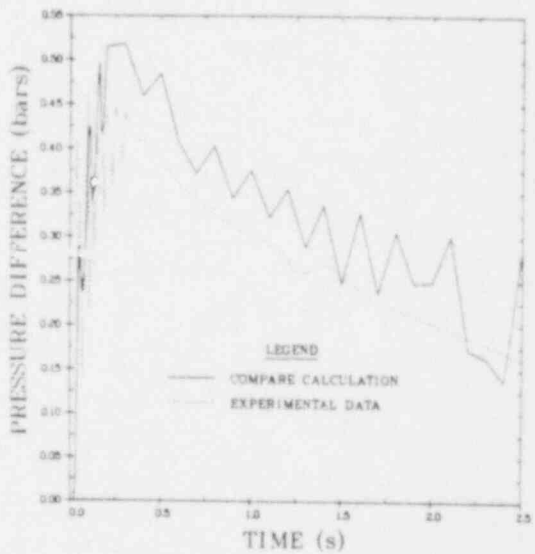

Fig. A-70. Comparison of COMPARE MOD-1 calculation with experimental data for test D15, room 6 to 4 differential pressure.

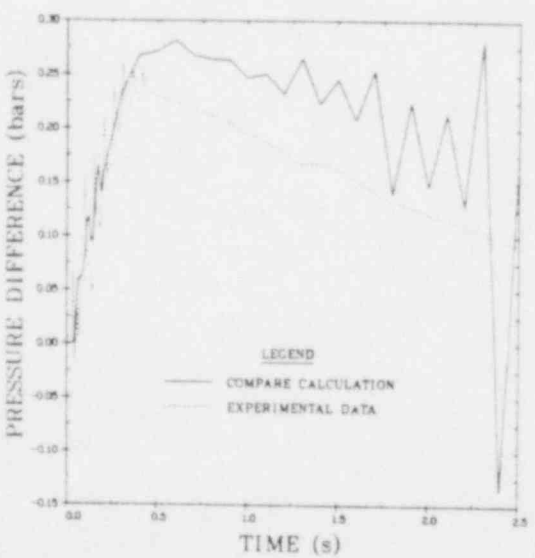

Fig. A-71. Comparison of COMPARE MOD-1 calculation with experimental data for test D15, room 8 to 4 differential pressure.

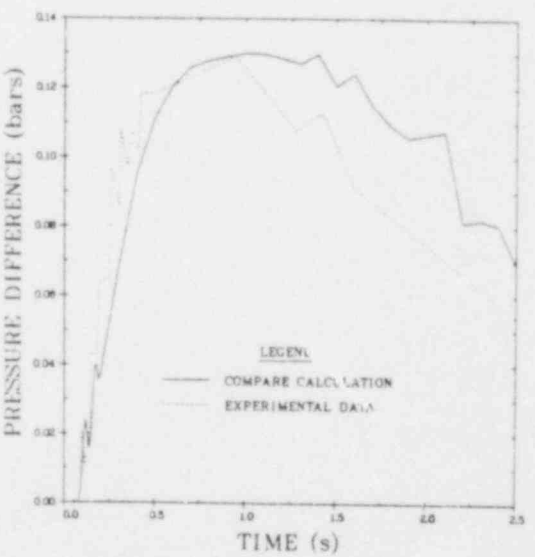

Fig. A-72. Comparison of COMPARE MOD-1 calculation with experimental data for test D15, room 7 to 4 differential pressure.

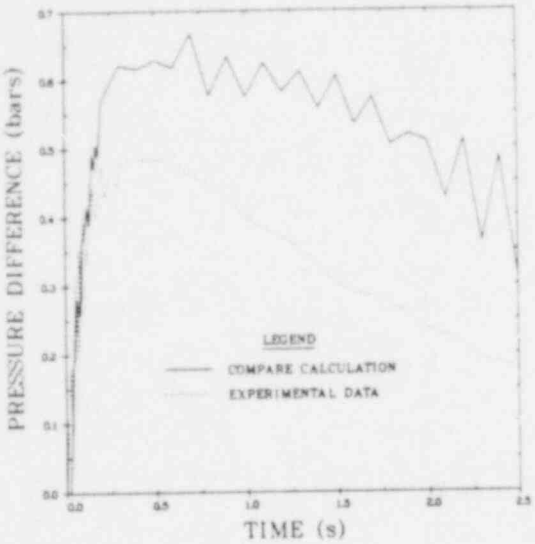

Fig. A-73. Comparison of COMPARE MOD-1 calculation with experimental data for test D15, room 6 to 9 differential pressure.

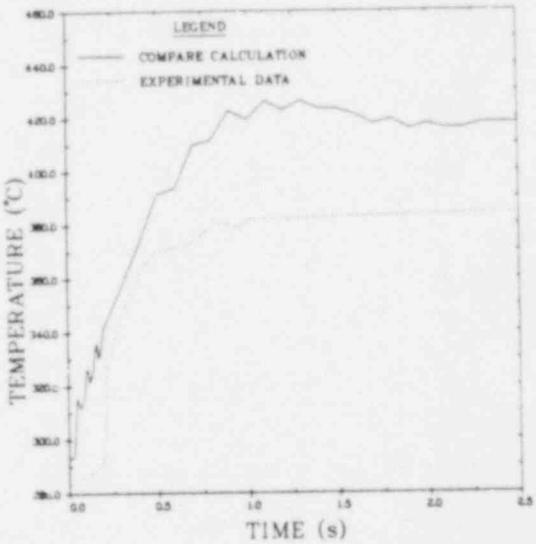

Fig. A-74. Comparison of COMPARE MOD-1 calculation with experimental data for test D15, room 6 temperature.

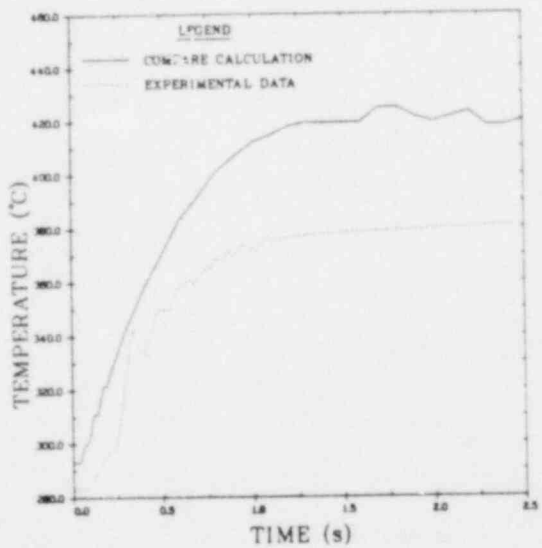

Fig. A-75. Comparison of COMPARE MOD-1 calculation with experimental data for test D15, room 8 temperature.

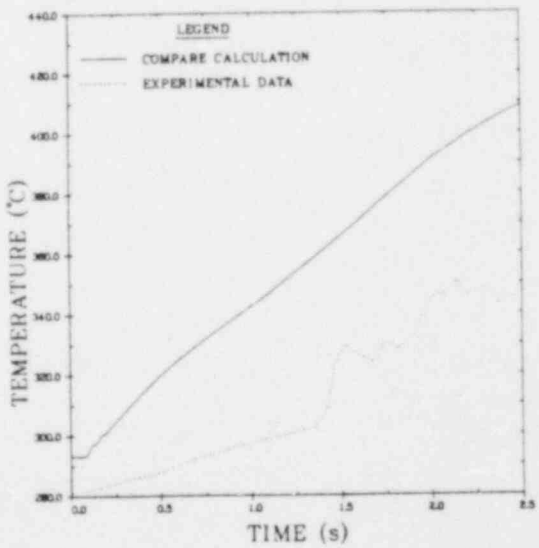

Fig. A-76. Comparison of COMPARE MOD-1 calculation with experimental data for test D15, room 7 temperature.

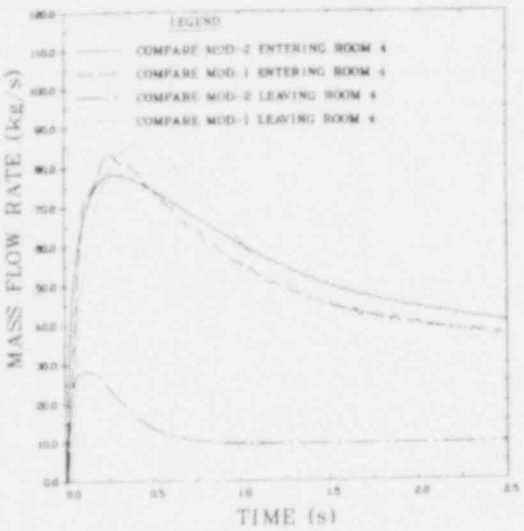

Fig. A-81. Comparison of COMPARE MOD-1, and COMPARE MOD-2 calculations of the nozzle mass flow rates entering and leaving room 4 for experiment D1.

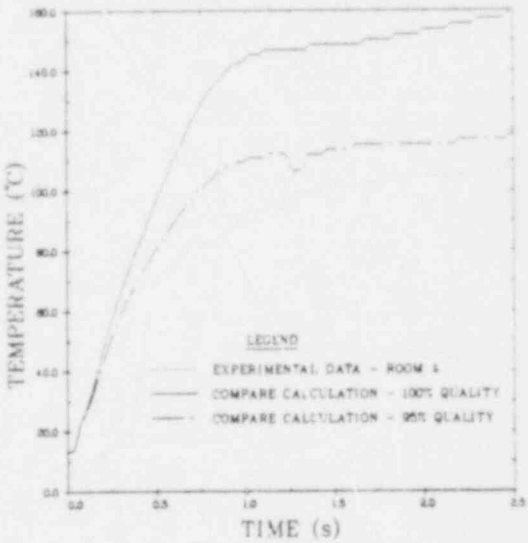

Fig. A-82. Sensitivity of room 4 temperature to the blowdown fluid quality.

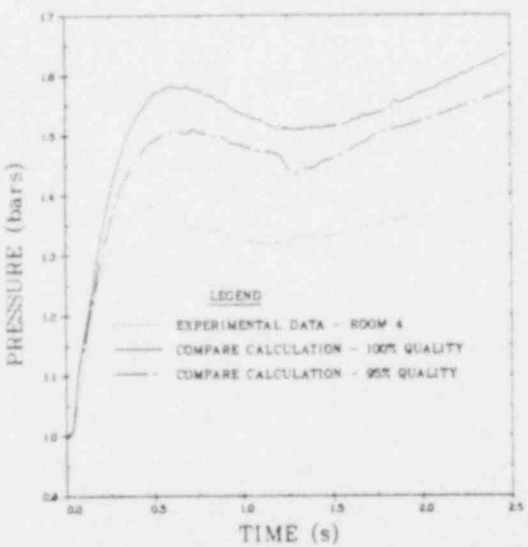

Fig. A-83. Sensitivity of room 4 pressure to the blowdown fluid quality.

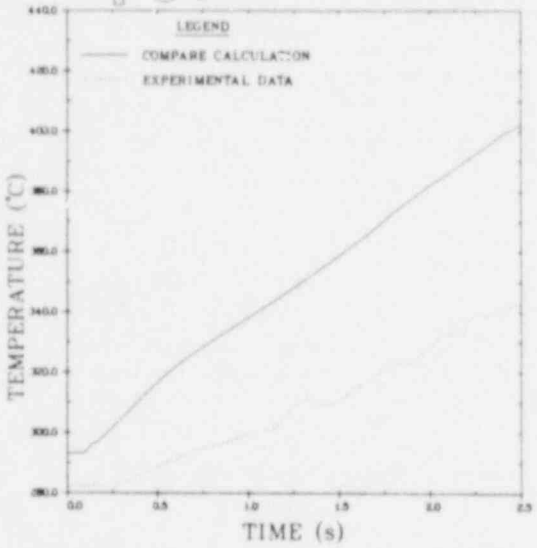

Fig. A-77. Comparison of COMPARE MOD-1 calculation with experimental data for test D15, room 4 temperature.

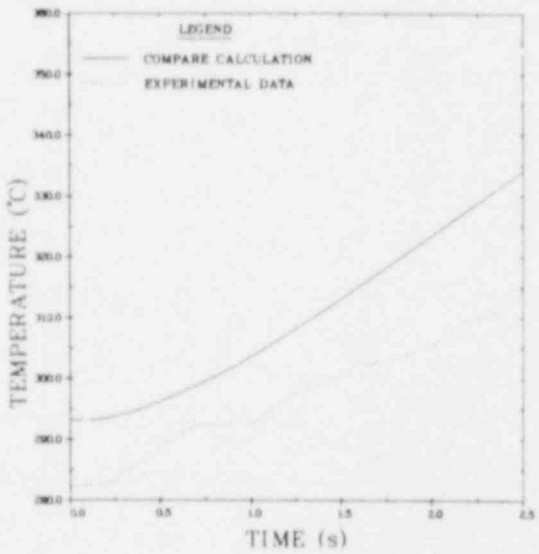

Fig. A-78. Comparison of COMPARE MOD-1 calculation with experimental data for test D15, room 9 temperature.

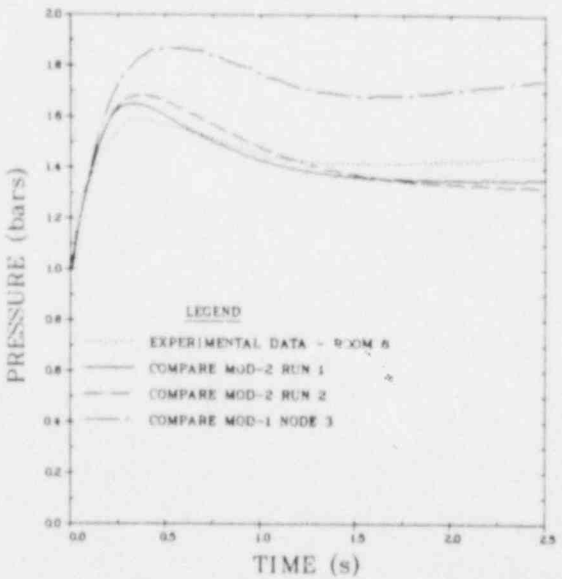

Fig. A-79. Comparison of COMPARE MOD-1, COMPARE MOD-2, and experimental data for test D1, room 6 pressure.

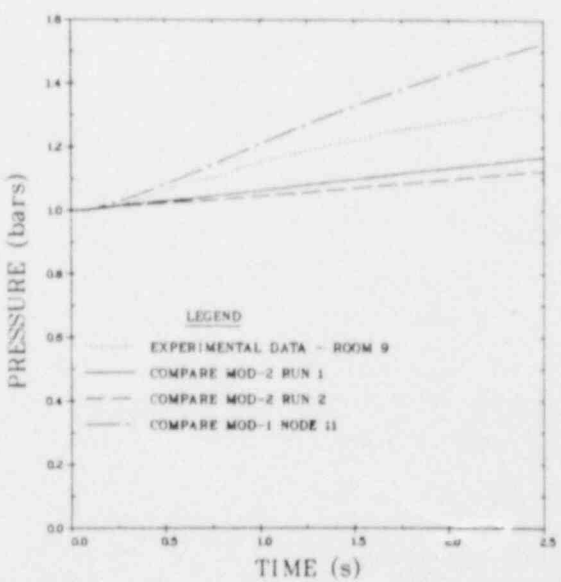

Fig. A-80. Comparison of COMPARE MOD-1, COMPARE MOD-2, and experimental data for test D1, room 9 pressure.

DISTRIBUTION

	Copies
Nuclear Regulatory Commission, R4, Bethesda, Maryland	388
Technical Information Center, Oak Ridge, Tennessee	2
Los Alamos National Laboratory, Los Alamos, New Mexico	50
	440

NRC FORM 335 (7 77)

U.S. NUCLEAR REGULATORY COMMISSION

BIBLIOGRAPHIC DATA SHEET

1. REPORT NUMBER (Assigned by DDC)
NUREG/CR-1817
LA-8615-MS

4. TITLE AND SUBTITLE (Add Volume No., if appropriate)
Comparison of COMPARE MOD-1 Subcompartment Calculations with Battelle-Frankfurt D-Series Test Results

2. (Leave blank)

3. RECIPIENT'S ACCESSION NO.

7. AUTHOR(S)
J.W. Bolstad, R.G. Gido, W.S. Gregory, P.E. Littleton, G.J. Willcutt, Jr.

5. DATE REPORT COMPLETED
MONTH: November YEAR: 1980

9. PERFORMING ORGANIZATION NAME AND MAILING ADDRESS (Include Zip Code)
Los Alamos Scientific Laboratory
P.O. Box 1663
Los Alamos, NM 87545

DATE REPORT ISSUED
MONTH: December YEAR: 1980

6. (Leave blank)

8. (Leave blank)

12. SPONSORING ORGANIZATION NAME AND MAILING ADDRESS (Include Zip Code)
Division of Systems Integration
Office of Nuclear Reactor Regulation
U.S. Nuclear Regulatory Commission
Washington, DC 20555

10. PROJECT/TASK/WORK UNIT NO.

11. CONTRACT NO.
FIN A7111

13. TYPE OF REPORT

PERIOD COVERED (Inclusive dates)

15. SUPPLEMENTARY NOTES

14. (Leave blank)

16. ABSTRACT (200 words or less)

This report describes the results of calculations performed with the COMPARE MOD-1 and COMPARE MOD-2 computer codes. The calculations were performed for six of the Battelle-Frankfurt D-series experiments. The main emphasis of the study is to present a comparison of calculated results and experimental data. The system models used are based on regulatory rather than best-estimate assumptions. The Battelle-Frankfurt D-series tests are described and complete noding information is given for experiments D1, D6, D9, D11, D14, and D15. The main features distinguishing these tests from the others are described. Detailed comparisons between COMPARE MOD-1 calculations and experimental data are given for absolute pressure, differential pressure, and temperature at various points in the system. General trends in the comparisons are noted. Results using a method-of-characteristics approach (COMPARE MOD-2) are presented for experiment D1. These results are compared with both the MOD-1 and experimental data. Summaries of parametric studies performed using COMPARE, aw well as studies performed by others, are described for the D-series experiments. Recommendations are given for assessing the conservatism in the calculations.

17. KEY WORDS AND DOCUMENT ANALYSIS

17a. DESCRIPTORS

17b. IDENTIFIERS/OPEN-ENDED TERMS

18. AVAILABILITY STATEMENT
Unlimited

19. SECURITY CLASS (This report)
Unclassified

21. NO. OF PAGES

20. SECURITY CLASS (This page)
Unclassified

22. PRICE
$

NRC FORM 335 (7 77)